DEPARTMENT OF THEORETICAL PHYSICS AND COMPUTER MODELLING

Head of Department *Dr. hab. phys.* Eugene Kotomin

Research Area and Main Problems

Our theoretical research interests are focused on six classes of problems related to:

- kinetics of diffusion-controlled processes, with emphasis on pattern formation and catalytic surface reactions;
- the atomic and electronic structure of numerous advanced materials, with emphasis on calculations of properties of defects, surfaces, metal/insulator interfaces.
- theoretical simulations and experimental studies of nanostructures and nanomaterials;
- modeling of advanced functional materials for energy applications (fuel cells, ceramic membranes, Li batteries, fusion and fission reactors);
- stochastization of magnetic field lines in magnetized fusion plasma;
- gyrotron development for thermonuclear reactors .

We combine several different techniques, including analytical formalisms and large-scale computer simulations (quantum chemical methods, stochastic simulations as well as Monte Carlo/cellular automata modeling)—for more details see our homepage http://www1.cfi.lu.lv/teor

Staff

Laboratory of kinetics in self-organizing systems	Laboratory of computer modeling of electronic structure of solids
Dr. O. Dumbrajs	J. Begens
Dr. D. Gryaznov	Dr. D. Bocharov
Dr. V. Kashcheyevs	Dr. R. Eglitis
Dr. E. Klotins	Msc. A. Gopejenko
Dr. hab. E. Kotomin	J. Kazerovskis
Dr.hab. V. Kuzovkov	Bsc. O. Lisovski
Msc. P. Merzlakovs	Dr. Yu. Mastrikov
Dr. A. Popov	Dr. S. Piskunov
Mcs. J. Sirmane	Dr. hab. Yu. Shunin
Dr. G. Zvejnieks	Bsc. A. Sorokin
	Dr. Yu. Zhukovskii

Scientific visits abroad

1. Dr. hab. E. Kotomin, Max-Planck Institut für Festkörperforschung, Stuttgart, Germany (9 months)
2. Dr. O. Dumbrajs, Max-Planck Institut für Plasmaphysik, Garching, Germany (2 month), Fukui University, Fukui (3 months)
3. Dr. D. Gryaznov, Max-Planck Institut für Festkörperforschung, Stuttgart, Germany (9 months); University College London (1,5 months)
4. Dr hab. V. Kuzovkov, Northwesten University, USA (3 months)
5. Dr. A. Popov, Deutsches Elektronen-Synchrotron DESY, Hamburg, Germany (3 weeks), Laue-Langevin Institute, Grenoble, France (1 month), Electronic Materials Division, Institute of Materials Science, Darmstadt University of Technology, Darmstadt, Germany (2 months)
6. Dr. D. Bocharov, Deutsches Elektronen-Synchrotron DESY, Hamburg, Germany (1,5 weeks)
7. A. Gopejenko, Institute for Applied Materials, Karlsruhe Institute of Technology , Karlsruhe, Germany (5 weeks)
8. O. Lisovski, Uppsala University, Sweden (4 months)
9. Dr. Yu. Mastrikov, Institute of Applied Materials, Karlsruhe, Germany (6 weeks)
10. Dr. S. Piskunov, University of Duisburg-Essen, Germany (2 weeks), Laboratori Nationali di Frascati, Italy (7 weeks); Institute of General and Inorganic Chemistry, Moscow (2 weeks)
11. Dr. hab. Yu. Shunin, Laboratori Nationali di Frascati, Italy (5 weeks)
12. Dr. Yu. Zhukovskii, St. Petersburg State University, Russia (1 month), Institute of Applied Materials, Karlsruhe, Germany (1 month), Institute of General and Inorganic Chemistry, Russian Academy of Science, Moscow (2 weeks).

International Cooperation

Belarus	1. Belarusian State University (Prof. S.A. Maksimenko)
Finland	2. Helsinki University of Technology (Dr. T. Kurki-Suonio)
France	3. Laue-Langevin Institute, Grenoble (Dr. G.J. McIntyre, Dr. H. Schober)
Germany	4. Max Planck Institut für Festkörperforschung, Stuttgart (Prof. Dr. J. Maier) 5. Deutsches Elektronen-Synchrotron DESY, Hamburg (Dr. A. Kotlov) 6. EC Institute of Transuranium Elements, Karlsruhe (Dr. P. Van Uffelen). 7. Max Planck Institut für Plasmaphysik, Garching (Dr. V. Igochine, Prof. Dr. K. Lackner, Dr. R. Mayer-Spasche, Prof. Dr. H. Zohm) 8. Institut für Hochleistungsimpuls & Mikrowellentechnik (KIT), Karlsruhe (Dr. S. Kern, Dr. B. Piosczyk) 13. Institut für Angewandte Materialien, Karlsruhe (Dr. A. Möslang) 14. Department of Theoretical Chemistry, University of Duisburg-Essen, (Prof. E. Spohr)

Greece	11. School of Electrical and Computer Engineering, National Technical University of Athens, Zographou (Dr. K. Avramides)
Israel	12. Ben Gurion University, Beer Sheeva (Prof. A. Aharony, Prof. D. Fuks)
Italy	13. Laboratori Nazionali di Frascati (Dr. S. Bellucci, Dr. M. Cestelli-Guidi)
Kazakhstan	14. Gumilyov National University, Astana (Prof. A. Akilbekov)
Japan	15. FIR Center, University of Fukui (Prof. T. Idehara)
Lithuania	16. Institute of Semiconductor Physics (SPI), Vilnius (Dr. E. Tornau)
Poland	17. Warsaw University, Dept of Chemistry (Dr A. Huczko)
Romania	18. University of Craiova (Dr. D. Constantinescu)
Russia	19. St. Petersburg State University (Prof. R.A. Evarestov) 20. Institute of General and Inorganic Chemistry, Russian Academy of Sciences, Moscow (Prof. P.N. Dyachkov)
UK	21. University College London (Prof. A.L. Shluger)
Ukraine	22. National University of Lviv (Prof. A. Voloshinovskii) 23. Institute for Scintillator Materials, Kharkov (Prof. A. Gektin)
USA	24. Northwestern University, Evanston, Illinois (Prof. M.Olvera de la Cruz) 25. University of Maryland, College Park (Dr. G.S. Nusinovich, Dr. M.M. Kukla)

Main Results

A. Electronic structure calculations for advanced materials

THE INTRINSIC DEFECTS, DISORDERING AND STRUCTURAL INSTABILITY OF $Ba_xSr_{1-x}Co_yFe_{1-y}O_{3-\delta}$ PEROVSKITE SOLID SOLUTIONS

E. A. Kotomin, Yu. A. Mastrikov,
M.M. Kuklja, B. Jansang (Materials Science Dept., University of Maryland, USA)
R. Merkle, J. Maier (Max-Planck-Institute for Solid State Research, Stuttgart, Germany)

Among many novel advanced materials for ecologically clean energy, ABO_3-type cubic perovskite solid solutions, e.g. $Ba_xSr_{1-x}Co_{1-y}Fe_yO_{3-\delta}$ (BSCF), are currently considered to be one of the most promising for applications as cathodes in solid oxide fuel cells (SOFC), oxygen permeation membranes, and oxygen evolution catalysis. These perovskites exhibit good oxygen exchange performance, the highest oxygen permeation rates known for a solid oxide, and mixed ionic and electronic conductivity. The low oxygen vacancy formation energy that is characteristic in these perovskites leads to the high oxygen vacancy concentration, and the relatively low activation barrier for the vacancy diffusion causes the high ionic mobility. These factors largely define the fast oxygen reduction chemistry of these materials which makes them such good candidates for energy conversion. However, a serious disadvantage of BSCF is its slow transformation at intermediate temperatures into a mixture of several phases, including a hexagonal phase with strongly reduced performance.

The basic properties of these perovskites and their stability with respect to decomposition into several phases are governed by structural defects and disordering. Detailed information regarding defect-induced effects, even in "simple" parent ABO_3 perovskites, with the sole exception of oxygen vacancies, is largely lacking thus far because these materials are extraordinarily complex and especially difficult to tackle experimentally. Hence, our understanding of the structure-property-function relationship in BSCF and similar materials is still far from comprehensive, which significantly hampers the progress in energy research and limits prospects to enhance existing materials or design new materials to improve efficiency of energy conversion devices.

In our research, a set of point defects: all types of single vacancies, Frenkel and Schottky disorder, and cation exchange, were explored in BSCF by means of first principles density functional theory (DFT) calculations. Configurations and energies of those defects were carefully characterized and discussed in the context of available experimental data. We focused on the defect energetics. It is confirmed that an oxygen vacancy has the lowest formation energy among all single vacancies probed. It is also established that oxygen Frenkel defects, full Schottky disorder and partial Schottky disorder accompanied by the growth of a new phase (e.g. a binary oxide) all have relatively low formation energies and are favorable. The obtained cation exchange energies are very low on both the A- and B-sublattices of the perovskite structure, which carries implications as to the stability of the materials and ultimately to the efficiency of energy conversion

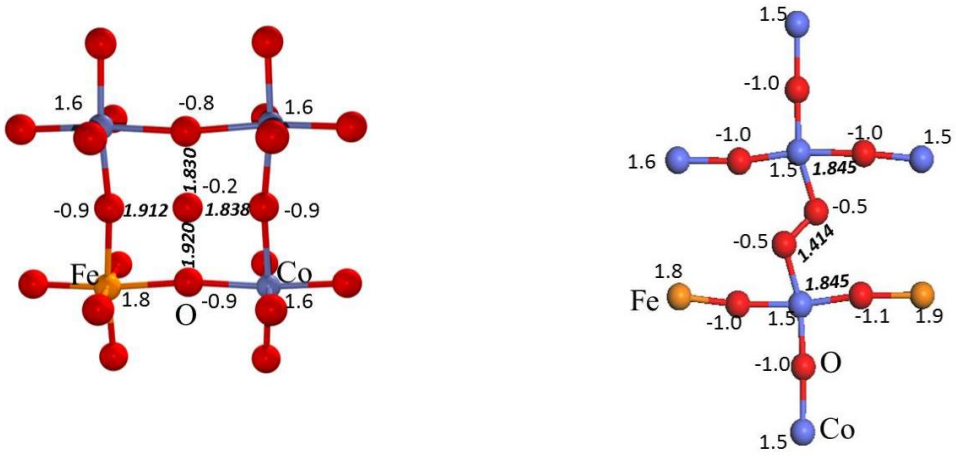

Fig. 1 Co-O-Co oxygen hollow (left) and split (right) interstitial configurations, their atomic charges, and inter-atomic distances.

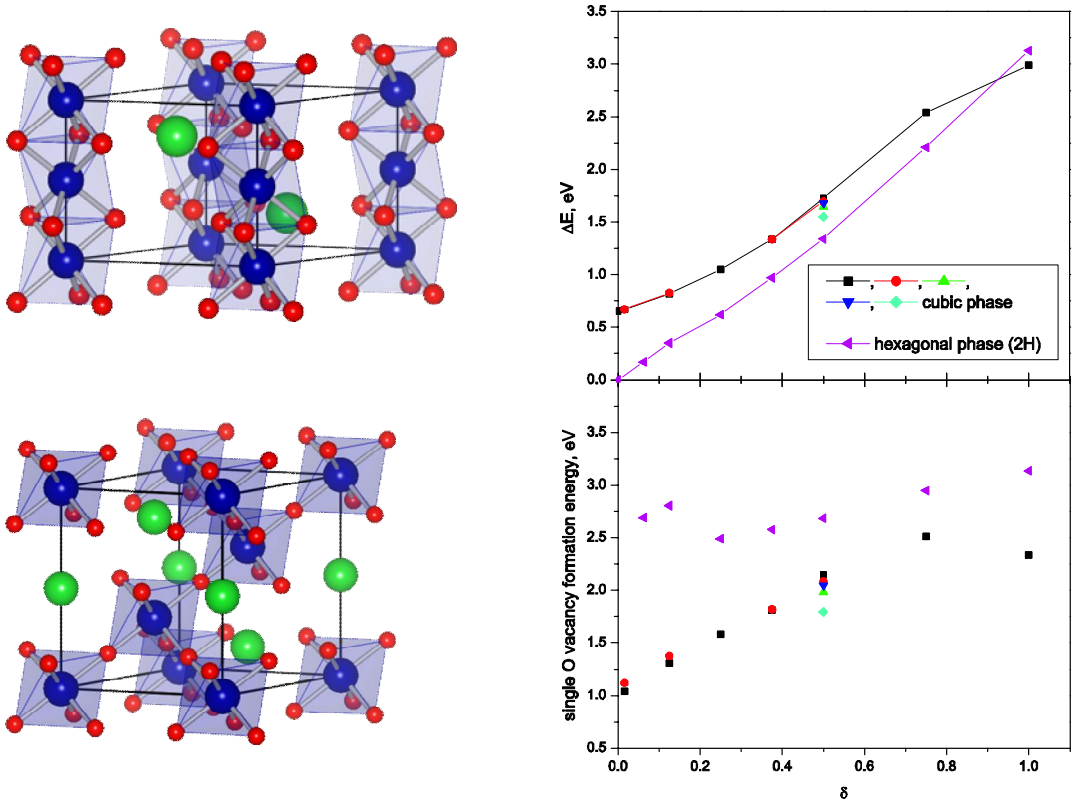

Fig.2 The cubic (left top) and the hexagonal (2H) (left bottom) BSCF structures are presented. Right- the total energy and the single vacancy formation energy of the cubic and hexagonal phases of BSCF are shown as a function of oxygen non-stoichiometry parameter δ. The total energies are given with respect to the stoichiometric hexagonal phase BSCF unit cell, which is 0.66 eV lower than the cubic phase unit cell. Five points shown for δ=0.5 demonstrate the energy dispersion depending upon a distribution of vacancies in the crystal.

HYBRID DFT CALCULATIONS ON GRAIN BOUNDARIES IN $BaZrO_3$

D. Gryaznov,
A.L. Shluger (University College London, UK)

In cooperation with the University College London, we performed the density functional theory (DFT) calculations on the properties of grain boundaries in proton conducting $BaZrO_3$. A blocking character of grain boundaries here has been reported affecting its transport properties. Thus, the main objective of the present study was to compare the properties of grain boundaries (GB) and vacancies behaviour in cubic perovskite $BaZrO_3$ with two methods, namely standard PBE and hybrid PBE0 exchange-correlation functionals. The calculations were done on a supercomputer facility at Edinburgh

University. A plane wave computer code VASP for the PBE functional and LCAO (linear combination of atomic orbitals) CRYSTAL09 code for the PBE0 functional were used. The former has been shown to be an effective tool whereas the latter code was used for the first within the present project for calculations of grain boundaries in oxides.

At the first stage, the bulk phase of $BaZrO_3$ was treated which included the calculation of density of states and oxygen vacancy formation energy using the two exchange-correlation functionals. As known for many oxides, the standard DFT (GGA/LDA) functionals underestimate their band gap. It then produces significant errors in the calculated properties. In order to solve this problem, one should go beyond the standard DFT functionals and use, for example, hybrid functionals. Also in the present study the band gap from the PBE0 functional was 4.9 eV (fig. 3) for bulk $BaZrO_3$, being well comparable to the experimental value of 5.0 eV. The band gap from the PBE functional was by 1.8 eV smaller than the experimental value.

The calculations of oxygen vacancy formation energy in the neutral supercell 2x2x2 (the concentration of oxygen vacancies 12.5%) gave 7.02 and 6.54 eV for the PBE0 and PBE functional, respectively. Note that the formation energies were calculated with respect to the energy of oxygen atom in the O_2 molecule (oxygen–rich conditions).

At the second stage, the same methods and functionals were used to calculate the properties of GBs in $BaZrO_3$ including the oxygen vacancy formation energy. In this case the calculations were at fixed (bulk) volume of the lattice but for the relaxed atomic coordinates. The GB was built in the supercell with the help of builder software on periodic models of CSL boundaries GBstudio. Supercells containing symmetric (310) [001] $\Sigma 5$ tilt GBs (misorientation angle 36.86^0) were constructed and contained 120 and 360 atom. The lengths of the supercell vectors were 10, 16 (32) and 19 (28) Å for 120 (360) atoms supercells. We have observed the presence of additional electronic states (mainly due to O p-electrons) in the band gap for the GB without the translation of one grain with respect to the other one (GB1 in fig. 1) using both the functionals and independently of the supercell size. Such electronic states are at different positions in the band gap for the two functionals as they are much closer to the top of valence band for PBE in comparison with PBE0. However, we have observed that the GB1 is not most energetically favourable. Therefore, the GB with translation (0.5 Å in the direction parallel with the GB) suggested not only lower GB energy but also no additional electronic states in the band gap (GB2 in fig. 3). The analysis of the density states for the GB1 with oxygen vacancy revealed the electronic states close to the bottom of conduction band. It was so far possible to calculate this GB for PBE only. We, thus, emphasize the importance of the choice of exchange-correlation functional and careful treatment of GB structure relaxation for the first-principle prediction of GB properties.

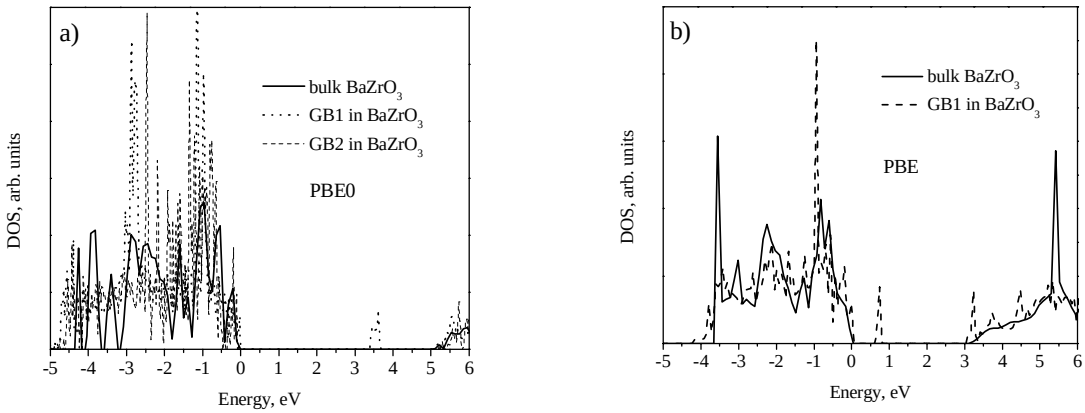

Fig. 3. The total density of states calculated for bulk and grain boundary of $BaZrO_3$ with PBE0 (CRYSTAL) and PBE (VASP) exchange-correlation functionals.

Ab initio CALCULATIONS OF DEFECTS ON MeF_2 AND $SrZrO_3$ SURFACES

R.I. Eglitis

The electronic *F*- and *R* centers in CaF_2 fluorite crystals have been studied using density functional theory (DFT) with a hybrid B3PW functional for of exchange and correlation effects. We estimated the *F*-center diffusion barrier as 1.7 eV. During the *F*-center jump, the trapped electron is more delocalized than that in the regular *F*-center case, and the gap between defect level and CB in the α-spin state decreases. The surface *F*-center investigation shows the energy preference for the *F* centers to locate near the surface. The association energy calculations of *R* centers indicate energy preference for aggregation of isolated *F* centers. During such the *F*-center aggregation, a considerable chemical bond covalency arises between two neighboring fluorine vacancies with trapped electrons. Three incompletely paired electrons trapped at the *R* center have an up-down-up spin arrangement and induce three defect levels in the gap between valence bands (VB) and conduction bands (CB) for both the α- and β-spin polarized band structures, respectively. More defect bands lead to more complex electron transitions, which were classified into two *F*- and four *M*-like transitions.

OH^- radicals in CaF_2 and BaF_2 bulk crystals and on the (111) surfaces have been studied as well. Three bulk and 20 surface OH^- configurations were investigated, and the energetically most favorable configurations detected. For the (111) CaF_2 surface atomic layers, the surface hydroxyls lead to a remarkable *XY*-translation and a dilating effect in the *Z*-direction, overcoming the surface shrinking effect in the perfect slab. The chemical bond population analysis shows a considerable covalency between the oxygen and hydrogen atoms, and the surface effect strengthens the covalency of surface OH^- impurities. There are two defect levels induced by OH^- impurities. The O 2p orbitals form two superposed

occupied O bands, located above the valence bands (VBs), and the H s orbitals do the major contribution to an empty H band, located below the conduction bands. Because of the surface effect, the O bands move downward, toward the VBs with respect to the relevant bands in the bulk case, and this leads to narrowing of the VB → O gap and widening of the O → H gap which corresponds to the first optical absorption.

We calculated also the surface relaxation and energetics for the polar (111) surface of $SrZrO_3$ with both Zr- and SrO_3-terminations. In both cases upper layer atoms are relaxed inwards. The second layer atoms, with the sole exception of Zr-terminated $SrZrO_3$ (111) surface Sr atom, relax outwards. The calculated surface relaxation energy for Zr-terminated $SrZrO_3$ (111) surface is almost 16x larger, than the surface relaxation energy for SrO_3-terminated $SrZrO_3$ (111) surface. The surface energy for Zr-terminated $SrZrO_3$ (111) surface is smaller, than that for for SrO_3-terminated one.

ELECTRONIC CHARGE REDISTRIBUTION IN $LaAlO_3$(001) THIN DEPOSITED AT $SrTiO_3$(001) SUBSTRATE: FIRST-PRINCIPLES ANALYSIS AND A ROLE OF STOICHIOMETRY

A. Sorokine, D. Bocharov, S. Piskunov, and V. Kashcheyevs

The discovery of conducting interface between two insulating materials: TiO_2-terminated (001) surface of $SrTiO_3$ (STO) substrate and $LaAlO_3$ (LAO) film deposited atop of it, has attracted colossal scientific interest during the last few years. Recently, high application potential of LAO/STO heterointerfaces has been proven *e.g.* by fabrication of highly voltage-tunable oxide diode that utilizes the advantage of the electric-field controlled interfacial metal-insulator transition of LAO/STO. Despite intense research efforts the origin of the charge carriers and the structure of the LAO/STO conducting layer are still controversially discussed. Currently, the whole picture responsible for adequate interpretation of experimental observations going in line with theoretical predictions is not yet clear. One of particular reasons for that is the fact that the major number of first principles studies carried out to describe structural and electronic properties of LAO/STO interfaces assume that the LAO films are perfectly stoichiometric. However, both pulsed laser deposition and molecular beam epitaxy vaporization processes used to facilitate transfer through the vapor LAO phase cannot preserve the target stoichiometry during LAO/STO synthesis. Taking into account that in fact La/Al ratio of nonstoichiometric LAO films may be controlled during its epitaxial growth, in our study we eliminate the above mentioned drawback by considering from first principles both n-LAO/STO and p-LAO/STO heterointerfaces having La or Al nonstoihiometry.

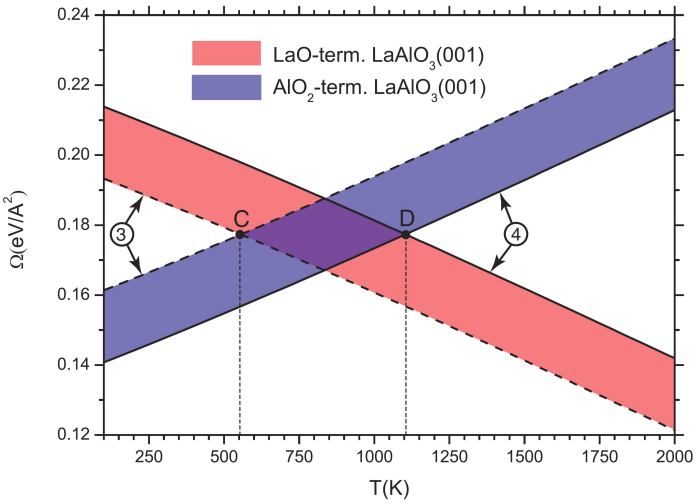

Fig. 4. The thermodynamic stability diagram calculated along the La_2O_3 and Al_2O_3 precipitation lines (numbers 3 and 4 in the circles, respectively. The dependence on the oxygen chemical potential is converted to the appropriate temperature scale at an oxygen pressure typical during LAO/STO(001) synthesis (P = 10^{-6} mbar). The interval between points C and D correspond to temperature range where both LaO- and AlO_2-terminated LAO(001) surfaces are stable and may coexist.

In general, in collaboration with *Faculty of Computing, University of Latvia*, we have performed large-scale first-principles calculations on a number of both stoichiometric and nonstoichiometric LAO/STO(001) heterostructures. We predict that there exists a distortion in energies of band edges for stoichiometric structures which eventually leads to the appearance of the conductivity at a critical thickness in *n*-type interfaces or to the reduction of the band gap for *p*-type interfaces. Nonstoichiometric interfaces were found to be conducting independently of the LAO film thickness and possessing little or no distortion of band edges. The conductivity appears due to the nonstoichiometry of the thin film which is a conductor on its own. The degree of distortion of the band edges agree well with the estimates of the internal electric field generated by changes in the atomic charges and the geometric relaxation of the atomic structure. We confirm these factors as the ones responsible for the rise of conductivity in stoichiometric *n*-type heterostructures.
Thermodynamic analysis that we have performed for the pristine LAO(001) surface reveals that both its LaO and AlO_2 terminations may coexist at temperatures above 550 K (Fig. 4). If the LAO/STO(001) heterointerface is covered by a LaO monolayer, charge compensation mechanism of deposited polar nonstoichiometric LAO film leads to the tendency of Ti^{3+} formation at the interface. In general, we conclude that one should not disregard the stoichiometry aspect when considering ways to make the LAO/STO interfaces conducting as nonstoichiometric interfaces possess unique quasi-2D electron gas structure that gives an overall 2 times greater free charge carrier density in comparison with stoichiometric interfaces. For stoichiometric *n*-type structures, the interplay of covalent and electrostatic forces leads to a metal-insulator transition at critical film thickness but, for nonstoichiometric structures, it leads to the formation of a bilayered or monolayered quasi-2D electron gas.

Ab initio CALCULATIONS OF S-doped TiO_2-NANOTUBE FOR PHOTOCATALYTICAL WATER SPLITTING APPLICATION

S. Piskunov, Yu. F. Zhukovskii, O. Lisovski

Solar energy has the capacity to fulfill global human energy demands in an environmentally and socially responsible manner provided efficient, low-cost systems which can be developed for its capture, conversion, and storage. Toward these ends, hydrogen fuel production from sunlight using semiconductor photocatalysts is a promising route for harvesting solar energy. Conventional photocatalytic electrodes such as titanium dioxide that use sunlight to split water and produce hydrogen can operate with high efficiency under ultraviolet irradiation, but it remains a challenge of primary importance, to drive them with visible light. Engineering the electronic energy band structure of nanostructured semiconductor photoelectrodes through judicious control of their atomic composition is a promising route to increase photoresponse of visible light. A general route to obtain a visible-light-driven photocatalyst is to dope a lattice of semiconductor with a wide band gap by extraneous elements, thus creating a new optical absorption edge. In this respect, hollow nanotubes produced from semiconducting materials have some peculiar advantages, such as larger specific surface area, higher mechanical stability, integrity and unique shape with few interfacial grain boundaries, which promote charge transport and electron-hole pair separation. Using hybrid exchange-correlation functionals within the density functional theory we have simulated in this study defective structure of TiO_2 nanotubes (fig.5).

On the basis of the performed first principles calculations, we conclude that the presence of substitutional impurities significantly affects the band structure of TiO_2 nanotubes, which must be taken into account when constructing nanoelectronic devices based on these nanotubes. Changes in nanotube's electronic structure can be observed by optical and photoelectron spectroscopy methods, as well as by measuring electrical properties of the nanotubes. According to obtained results S dopant in TiO_2 nanotube create the mid-gap states making this nanotube to be good candidate for efficient photocatalysts working under daylight irradiation.

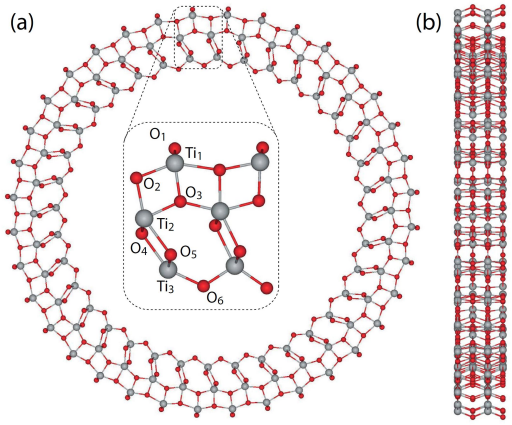

Fig. 5. Schematic representation of monoperiodically repeated unit cell of the substitutional defect containing (0,36) TiO_2 nanotube with external diameter of 4.81 nm: (a) across section view, (b) side view. Ti are shown as gray balls, while oxygen as red (light gray) ones. Inset shows the 2×2 increased "basic" unit cell of (0,36) TiO_2 nanotube repeated by 18 rototranslational symmetry operators (rotation axis of 18-th order). Numbered atoms of titans and oxygens are substituted for impurity defect atoms (A_h, where h stands for "host").

FIRST PRINCIPLES SIMULATIONS OF ELECTRONIC AND THERMODYNAMIC PROPERTIES OF DEFECTIVE ZnO

A.V. Sorokine, D. Gryaznov, Yu.F. Zhukovskii, J. Purans and E.A. Kotomin

We have performed large-scale calculations on electronic and thermodynamic properties of defective zinc oxide in its most stable phase at room temperature. Firstly, geometric and electronic bulk properties of ZnO single crystals have been considered and compared to experimental data. To improve the quality of obtained results, we have constructed new basis sets both for Zn and O. After consideration of various hybrid functionals we chose non-parametric PBE0 correlation-exchange functional for all the calculations, as it gave results both close to experimental data and stable with respect to change of computational parameters. Next,

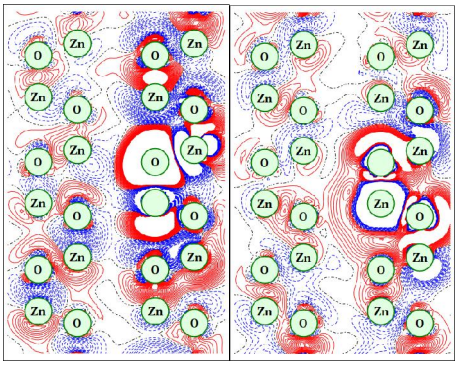

Fig. 6: Differential electronic charge density for ZnO with 6 % of vacancies of Zn (left) and O (right).

we considered intrinsic ZnO defects that are most likely to form in manufacturing processes: zinc and oxygen vacancies. Here we showed how electronic and geometric properties of defective structures change with the concentration of vacancies. For these calculations a supercell model was used, and the molar concentrations of defects were from 6 to 1.9 %, where the latter is an adequate result that can occur in experimental works. Electronic properties comprised atomic charges and differential electronic density. The latter is shown in Fig. 6.

We have also calculated defect formation Gibbs energy and its dependency on temperature and concentration of vacancies, as well as ZnO lattice vibrational phonon frequencies. Our results demonstrate how the V_O formation energy converges with the supercell size and the number of *k*-points for phonon calculations. The chemical potential of oxygen having the strongest effect for the formation energy changes its value from 4.1 eV down to 3.1 eV within a broad temperature range. Further the phonons in the solid phase produce additional effect of the order of 0.01 eV at $T = 0$ K and 0.03 eV at $T = 1000$ K. These estimations suggest that the temperature contribution to the V_O formation energy in ZnO comes from the chemical potential of oxygen.

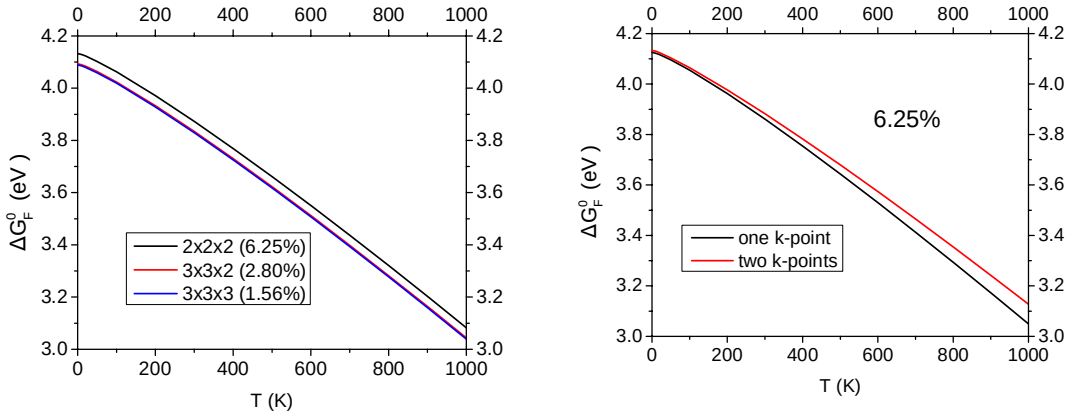

Fig. 7: Temperature effects through the chemical potential of oxygen only (left) and through the phonon contribution in solid and the chemical potential of oxygen (right).

FIRST-PRINCIPLES SIMULATIONS ON VARIOUS TYPES OF RUTILE-BASED TITANIA NANOWIRES AND THEIR STRUCTURAL ANALYSIS

Yu.F. Zhukovskii,
R.A. Evarestov (*Department of Quantum Chemistry, St. Petersburg University, Russia*),
D.B. Migas (*Belarusian University of Informatics and Radioelectronics, Minsk, Belarus)*

Within the rod group irreducible representations developed *in collaboration with Prof. R.A. Evarestov (St. Petersburg University, Russia) and Dr. D.B. Migas (Belarusian University of Informatics and Radioelectronics)* the one-periodic (1D) nanostructures have been considered for symmetry analysis of [001]- and [110]-oriented rutile-based titania

nanowires of diameters terminated by either four types of related {110} facets (Fig. 8) or alternating $\{1\bar{1}0\}$ and {001} facets (Fig. 9), respectively. Symmetry of nanowires has been described using both the Ti atom-centered rotation axes as well as the hollow site-centered axes passing through the interstitial sites between the Ti and O atoms closest to the axes. For simulations on TiO_2 NWs, we have performed large-scale *ab initio* Density Functional Theory (DFT) and hybrid DFT-Hartree Fock (DFT-HF) calculations with the total geometry optimization within the Generalized Gradient Approximation (GGA) in the form of the Perdew-Becke-Ernzenhof exchange-correlation functionals (PBE and PBE0, respectively), using the formalism of linear combination of localized atomic functions (LCAO) implemented in *CRYSTAL09* code. Both structural and electronic properties of enumerated rutile-based titania slabs and nanowires have been calculated.

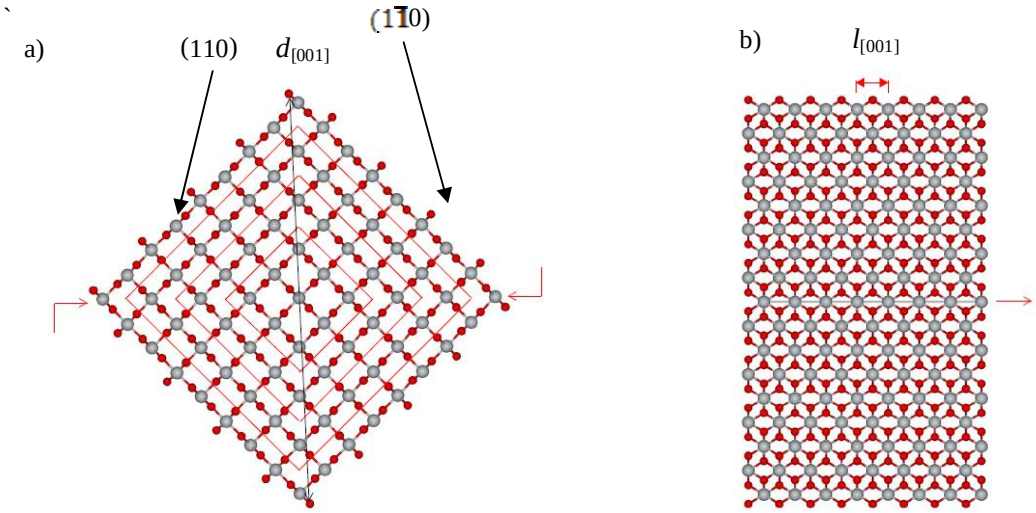

Fig. 8. Cross sectional (a) and lateral (b) images of non-optimized large rutile-based [001]-oriented Ti atom-centered nanowire possessing the D_{2h} symmetry and containing 81 formula units *per* NW unit cell with aside (110) and $(1\bar{1}0)$ facets shown in Fig. 8b. Red rhombs in Fig. 8a show borders for prism models of middle, small and smallest TiO_2 NWs (49, 25 and 9 formula units per UC, respectively). Diameter of a nanowire is shown by the twice-terminated arrow ($d_{[001]}$) while its period (length of UC) is shown in Fig. 8.b as $l_{[001]}$.

Nanowires are constructed as 1D systems cut from the 3D crystal along the direction of one of the bulk crystal symmetry axes. The translational periodicity is maintained along this direction. In the case of a rutile-based [001] TiO_2 nanowire (Fig. 8) a direction of the translation axis is orthogonal to a pair of [110] and $[1\bar{1}0]$ vectors while both titania formula units of primitive cell lie in the two cross-sectional planes. If the translational two-fold rotation axis goes through a Ti atom (Fig. 8), one can see that the reflection in the horizontal (*h*) plane and rotations around the two second order axes in this plane are the symmetry operations for [001]-oriented nanowires. The rod symmetry group of this system is *Pmmm* while its point symmetry group is D_{2h}.

For a rutile-based [110] nanowire (Fig. 9), the translation axis is orthogonal to [001] and $[1\bar{1}0]$ vectors while four formula units of primitive cell lie in the six cross-sectional planes. The

symmetry of a rutile-based [110] nanowire coincides with the symmetry of analogous type of [001] NW if the translation axis with rotation by π goes through Ti atoms. Indeed, Fig. 9, shows that the symmetry operations for [110] NWs are reflection in the vertical (v) plane (containing the translation axis) and rotation around the 2-fold translation axis in this plane. The symmetry operations include also rotations around the 2-fold axis in the horizontal (h) plane (orthogonal to the translation axis). Thus, the rod symmetry group of the system is again *Pmmm* (the point symmetry group is D_{2h}).

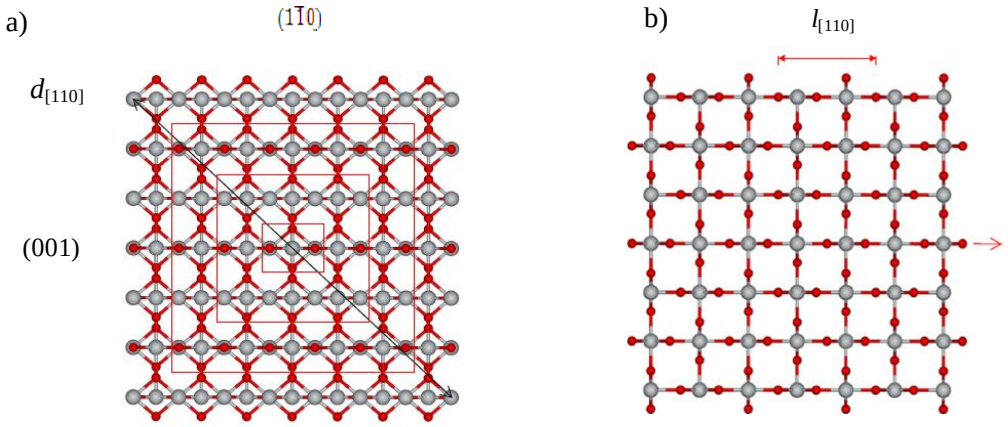

Fig. 9. Cross sectional (a) and lateral (b) images of the non-optimized large rutile-based [110]-oriented Ti atom-centered NW possessing the D_{2h} symmetry and containing 105 formula units per NW UC, with aside (001) and (1$\bar{1}$0) facets (the former is shown in Fig. 9.b). Rectangles in Fig. 9.a show borders for prism models of middle, small and smallest TiO_2 NWs (55, 21 and 3 formula units per UC, respectively). NW diameter is shown by the twice-terminated arrow ($d_{[110]}$) while its period (length of UC) is shown in Fig. 9.b as $l_{[110]}$.

The properties of titania nanowires are both the size and shape dependent. For direct comparison of relative stability of various 1D nanowires, we have performed large-scale calculations on their surface energy *per* formula unit. Values of d_{NW} slightly increase whereas l_{NW} are found to be reduced after NW geometry optimization. The larger is d_{NW}, the closer its geometry parameters as well as the band gap to those of rutile-based TiO_2 bulk and non-optimized (001) and (110) slabs whereas NW surface energy approaches to that of facets terminating the nanowire. In the case of Ti atom-centered NWs, values of $\Delta\varepsilon_g$ grow with increasing d_{NW} while in hollow site-centered NWs, these values decrease in analogous conditions, analogously to band gaps of slabs with increasing thickness.

THEORETICAL SIMULATIONS OF ELECTROMAGNTIC PROPERTIES IN CARBON NNTUBES AND GRAPHENE BASED NANOSTRUCTURES

Yu.N. Shunin, Yu.F. Zhukovskii,
S. Bellucci (*Laboratori Nazionali di Frascati, Italy*)

In collaboration with Dr. S. Bellucci (Laboratori Nazionali di Frascati, Italy), we have developed the model of *'effective bonds'* in the framework of both cluster approach based on the multiple scattering theory formalism and Landauer theory, which can allow us to

predict the resistivity properties for C-Me junctions taking into account chirality effects in the interconnects of single-wall (SW) and multi-wall (MW) CNTs (Fig. 10) as well as monolayer (ML) and polylayer (PL) GNRs (Fig. 11) with the fitting metals (Me= Ni, Cu, Ag, Pd, Pt, Au) on predefined geometry of carbon nanostructure.

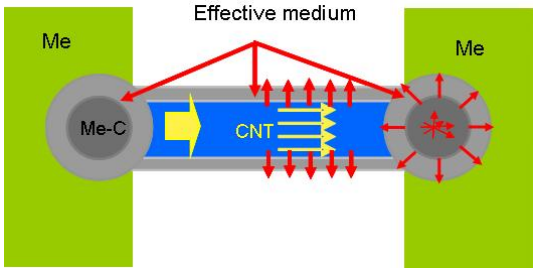

Fig. 10. Model of CNT - Me interconnect.

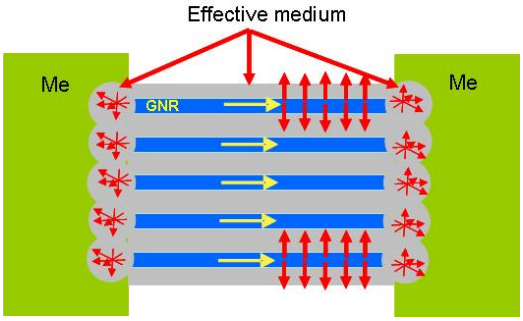

Fig. 11. GNR (polylayered) - Me interconnect.

We have also developed the concept of simulation of carbon based nanosensor devices. Interconnect capacitances and impedances have been evaluated in the GHz and THz regimes. Parametrical numerical simulations of conductivity have been carried out for zig-zag (*m*,0), arm-chair (*m*,*m*) and chiral (*m*,*n*) CNTs while the sensitivity of conductivity to the local electronic density of states in CNTs with local impurities (N and B atoms) has checked. CNTs, CNT-Me and GNR-Me based nanostructures are prospective nanosensor structures. Conductance and other current-voltaic parameters depend on the morphology of the nearest shells in MW CNTs and PL GNRs, which results in complications for technological synthesis. Nevertheless, the corresponding nanodevices possess the stable electrical characteristics.We have made a further step in simulations directed to nanosensor systems. In this respect, due to the sensitivity of the local electronic density of states to external influences (mechanical, chemical, electrical, magnetic, *etc*), the fundamental electromagnetic properties of CNTs, GNRs and their metal interconnects have been analyzed from the point of view of prospective nanosensor applications. We have created the database of CNT-metal and GNR-metal junction combinations taking into account a set of parameters, and namely, the angle of chirality, the CNT diameter, the number of walls or layers, the type of a metal substrate (Me), and the orientation of a metal substrate, *e.g.*, the densely-packed (100), (111) and (110) surfaces. Thus, we are able to forecast interconnect properties for various SW and MW CNT, ML and PL GNR configurations.

There are some important applications of CNT- and GNR-based interfaces with other materials for creation of novel nanosensor devices, *e.g.*, for design of prospective electron devices like FET-transistors (Fig. 12) which are very sensitive to various external influences of different nature as mentioned above.

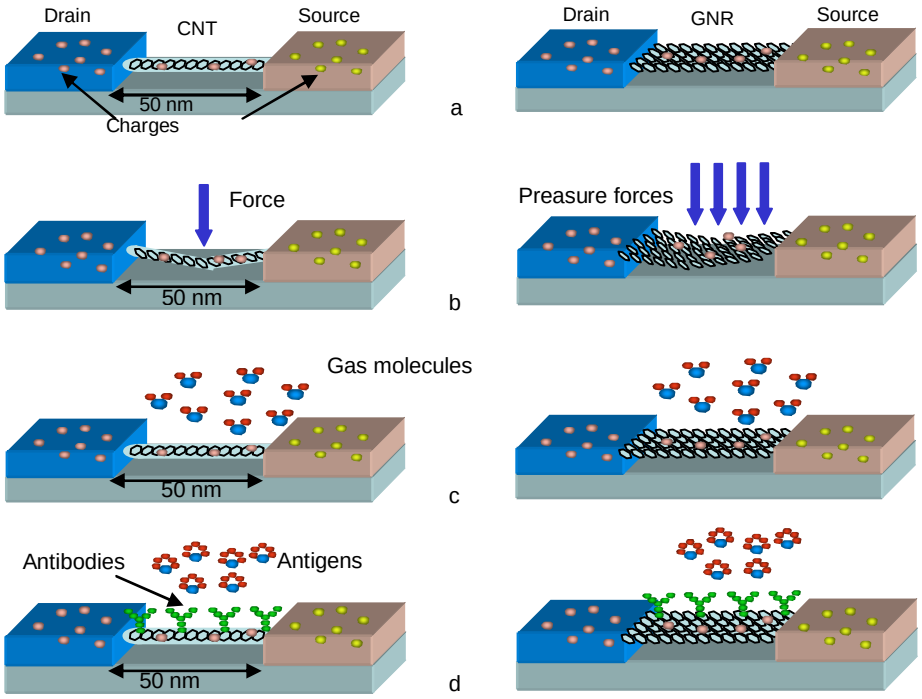

Fig.12. FET-type nanodevices as prospective nanosensor systems: a) the unperturbed field-effect transistors based on CNT and GNR are presented (CNT- or GNR- based FETs are mainly composed of the corresponding semiconducting carbon materials suspended over the two electrodes); b) physical nanosensors: a conducting threshold can be altered when the nanotube or graphene ribbon is bent; c) chemical nanosensors: this threshold can be altered when the amount of free charges on the nanotube of graphene ribbon surface is increased or decreased depending on the presence of donor or acceptor molecules of specific gases or composites; d) biological nanosensors: monitoring of biomolecular processes such as antibody/antigen interactions, DNA interactions, enzymatic interactions or cellular communication processes, *etc*.

Potential nanosensor devices based on CNTs and GNRs as well as their interconnects with various metallic electrodes are possible to design and to use for effective detection of external influences of different nature. They can change the electron transport regime and promote the current losses. At the same time, the interconnect interfaces can also be sensitive to chemical adsorbents, electrical and magnetic fields, changing the properties of interconnect potential barrier and the efficiency of conducting channels. Both these nanosensoring mechanisms can be simulated in the framework of the proposed models.

AB INITIO MODELLING OF OXYGEN INTERACTION WITH SURFACES AND INTERFACES OF URANIUM MONONITRIDE

D. Bocharov, D. Gryaznov, Yu.F Zhukovskii, E.A. Kotomin

In collaboration with *Institute for Transuranium Elements, Karlsruhe, Germany and Faculty of Computing, University of Latvia*, oxygen adsorption, migration, incorporation into the surface N vacancies on (001) and (110) surfaces as well as oxygen behaviour between UN grain boundaries have been modeled (Figs. 13 and 14) using 2D slabs of different thicknesses and supercell sizes and the GGA exchange-correlation functional PW91 as implemented in *VASP* code. The Gibbs free energies of N vacancy formation and O atom incorporation therein at the two densely-packed surfaces and tilt grain boundaries are compared.

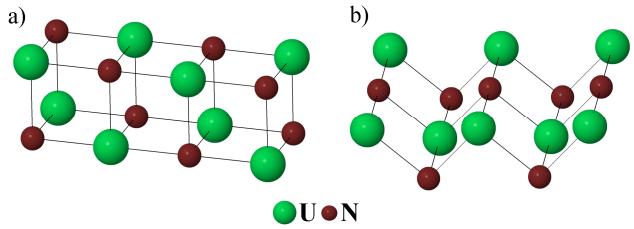

Fig. 13. The slab models for the UN (001) (a) and (110) (b) surfaces (only the two outermost layers are shown).

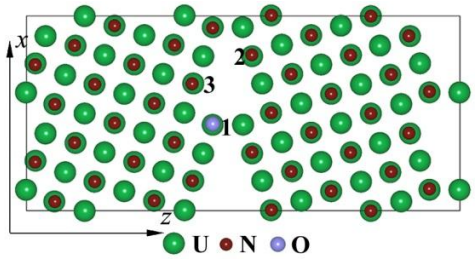

Fig. 14. The cross-section of the (310)[001](36.8°) tilt GB supercell [29] (15.40 Å × 4.87 Å × 34.13 Å with the oxygen atom incorporated into one of three possible positions.

The formation energies $E_{form}^{\mathrm{N\_vac}}$ of N vacancy at 0 K inside the GB are equal with 3.3-3.5 eV. These values are comparable with analogous values for $E_{form}^{\mathrm{N\_vac}}$ on UN (001) (3.6-3.7 eV) and (110) (2.9-3.1 eV) surface and are smaller than those in the bulk material (~4.4 eV) or in (001) or (110) slabs central layer (4.3-4.6 eV). It indicates a clear trend for segregation of vacancies towards the grain boundaries.

The standard *Gibbs free formation energy* as a function of temperature is plotted in fig. 15 for the two UN surfaces and grain boundary. The difference in the standard Gibbs free formation energy ΔG_F^N between the (001) and (110) surfaces is considerable, 0.7 eV (fig. 15) and, most importantly, ΔG_F^N decreases by 0.4 eV as the temperature increases from 400 to 700 K. The formation energy at the GB lies in-between that for the two surfaces. *Incorporation energy* ΔG_I^O negative values means that the reaction is exothermic and thermodynamically favorable. It *increases* with temperature by ~0.4 eV in the temperature range from 400 to 700 K but remains still negative (process energetically favorable).

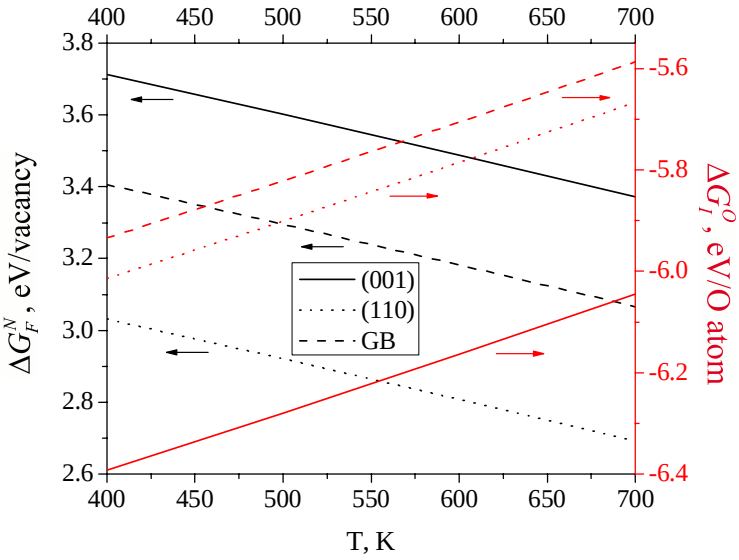

Fig. 15. The standard Gibbs free formation energy of N vacancy (black curves) and the incorporation energy of O atom into the surface N vacancy (red curves) as a function of temperature for the (001), (110) surfaces and GB (position 2 in Fig. 14). The supercell size and slab thickness are 3×3 and 7 planes, respectively.

The oxygen incorporation energy for the GB is smaller than for both surfaces, but remains still negative, even at 700 K. Lastly, the O solution energies (incorporating also N vacancy formation cost) in all three cases are predicted to be very close and negative (-2.5 eV), thus the oxidation process is energetically favorable at all studied temperatures that explains fast oxidation of UN on air.

FIRST PRINCPLES SIMULATIONS OF Y_2O_3 CLUSTER GROWTH IN ODS STEELS

A. Gopejenko, Yu.F. Zhukovskii, Yu.A. Mastrikov, E.A. Kotomin,
P.V. Vladimirov, A. Möslang (*Institut für Angewandte Chemie, KIT, Karlsruhe, Germany*)
V.A. Borodin (*Research Center Kurchatov Institute, Moscow, Russia*)

Reduced activation ferritic-martensitic steels (RAFM) strengthened by yttria precipitates are promising structure materials for future fusion and advanced fission reactors. Oxide dispersion strengthened (ODS) particles hinder dislocation motion effectively resulting in higher strength and better high-temperature creep resistance of ODS steels in comparison to basic materials. Implementation of ODS materials widen the operating temperature as compared to conventional RAFM steels as well as they are more radiation resistant. The size and spatial distribution of ODS nanoparticles significantly affect both mechanical properties and radiation resistance. Unfortunately the mechanism of the ODS particle formation is not completely understood.

In close collaboration with partners from *the Karsruhe Institute of Technology (Germany)* and from the *Kurchatov Institute, Moscow (Russia)*, we performed a computer modelling of the ODS particle formation process. Experimental studies, performed at the KIT, show that a significant part of Y and O atoms is found in the steel matrix in the concentrations exceed their equilibrium solubility after milling. Depending on Cr concentration, during the cooling process steel may or may not go through the phase transformation. Therefore, we consider the ODS particle formation process in both- *fcc* and *bcc*- phases. There is a significant lattice mismatch between the *fcc*/*bcc*-Fe and the bixbite-type Y_2O_3. At the very initial steps of the ODS particle formation process, space, necessary for creation the bixbite-type bonds within the iron matrix, could be provided by vacancies.

For the *fcc* phase, we found the most stable configuration of three vacancies and single Y atom. The lowest energy was obtained for the systems with the solute atom, located at the centre of the cluster. For the *bcc* phase we investigated the growth of vacancy cluster. The largest modelled cluster contained nine vacancies. The same process was repeated with a single Y atom. For all systems the binding energy increases with the number of vacancies, except adding the seventh vacancy. The interaction between Y atom, stabilized by divacancy with solute Y_{Fe} atom, at close distances is attractive. The largest attraction energies (1-1.1eV) are obtained for the systems with obtuse V_{Fe}-Y_i-V_{Fe}-Y_i-V_{Fe} angles. Two Y atoms, each stabilized by divacancy, attract to one another. For the first three NN spheres vacancies overlap. Without overlapping, for the nearest coordination spheres binding energy is about 1.3 eV.

The results of the calculations on both phases clearly show that Fe-vacancies play a major role in binding between defects. It was found for the *fcc* phase, that binding energy between Fe-vacancies significantly increases in the case of four vacancies in comparison to the configurations with two or three Fe vacancies. The largest binding energies were found for the configurations with a single Y atom and several vacancies. The binding energies for the configuration between two Y atoms and vacancy increase with the increase of the distance between two Y atoms, and in the case of the 4-NN attraction was observed between two Y atoms inside the lattice. In *bcc*-Fe, vacancies segregate, creating stable clusters. The growth of the Y_i ; $6V_{Fe}$ cluster is restricted by a barrier of, at least, 1.8 eV. Y_{Fe}, surrounded by $8V_{Fe}$ may slightly oscillate along the [111] and equivalent directions. The attraction between Y_{Fe} and Y_i; $2V_{Fe}$ cluster is about 1 eV. Two Y_i; $2V_{Fe}$ complexes binding energy is 1.2-1.4 eV. Stabilization of solute Y atoms by vacancies increases the binding energy between them.

QUANTUM-CHEMICAL STUDY OF ELECTRON-PHONON INTERACTIONS IN CRYSTALS

E. Klotins and G. Zvejnieks

A fundamental problem in solid state physics is to understand what happens when electrons couples to an atomic environment of and, in particular, what is the nature of electron – phonon interaction, and what is the mathematical framework decoupling this interaction. The associated theory is still incomplete and lacks two important components: a physical picture that clarifies how electrons emerge above their ground state under

electromagnetic radiation and the interaction with phonons, and a regular mathematical framework for studying these phenomena.

We investigate a minimal yet detailed model system that describes interacting electron gas moving in a charge compensating background of positive ions and interacting with external electromagnetic field.

The performed analysis suggests that for dielectrics and semiconductors modeled by effective Hamiltonians, the interaction with electromagnetic field comprises potentional energy terms additional to the conventional impact in the kinetic energy of electrons. Nevertheless, the Hamiltonian retains its second quantized form with additional terms compatible to the annihilation and creation operators, as advancement.

The electron-phonon interaction is more complex and is accounted for by a mixture of electronic and phonon birth/annihilation operators incompatible with the second quantization approach. This undesirable property is eliminated by Baker – Hausdorf transformation applicable to arbitrary electron – phonon interaction Hamiltonian and resulting in relations for the generator of this transformation and for the transformed electron-phonon interaction. This mathematical framework determines a starting point for an arbitrary effective Hamiltonian to decouple the electron-phonon interaction by transformation of a particular lattice Hamiltonian to the expected purely electronic secondary quantized two – particle interaction Hamiltonian compatible with the standard wave function and atomic orbital approaches.

VIBRATIONAL PROPERTIES OF $LaPO_4$ NANOPARTICLES IN MID- AND FAR-INFRARED DOMAIN

A. I. Popov, V. Pankratov,
P. Savchyn, V. Vistovskyy, A. Voloshinovskii, I. Karbovnyk (*I. Franko National University of Lviv, Ukraine)*
M. Cestelli, Guidi, C. Mirri (*INFN-Laboratori Nazionali di Frascati, Italy)*
O. Myahkota, A. Riabtseva, N. Mitina, A. Zaichenko *(Lviv Polytechnic National University, Ukraine)*

Lanthanum orthophosphate ($LaPO_4$), also known as monazite, has been widely used as a green phosphor, when doped with Ce and Tb in high-quality tricolour luminescent lamps. It has been used as a proton conductor, as well as in lasers, sensors, ceramic materials, catalysts, and heat resistant materials. This is due to its interesting properties, such as high thermal stability, very low solubility in water, high index of refraction, and so on. Nanopowders of $LaPO_4$ have been grown by sedimentation-micellar method. As-prepared $LaPO_4$ nanoparticles with the average grain size of about 8 nm have a single-phase hydrated hexagonal structure. After thermal annealing at 600 and 800 C, the average size of nanoparticles increases up to 35 and 50 nm, respectively, and the structure transforms into single-phase monoclinic. IR spectra of $LaPO_4$ nanoparticles of different size were investigated in the wide range of wavenumbers from 130 to 5000 cm^{-1} in the 20–300 K temperature region. Differences between IR spectra of the bulk material and nanoparticles as well as the temperature behavior of the vibrational properties are discussed.

SYNHROTRON RADIATION STUDIES ON LUMINESCENCE OF Eu^{2+}-DOPED $LaCl_3$ MICROCRYSTALS EMBEDDED INTO NaCl MATRIX

V. Pankratov, A.I. Popov
P.V. Savchyn, V.V. Vistovskyy, A.S. Voloshinovskii (I. Franko National University of Lviv, Ukraine)
A.S. Pushak (Ukrainian Academy of Printing, Lviv, Ukraine)
A.V. Gektin (Institute for Scintillation Materials NAS of Ukraine, Kharkov, Ukraine)

The divalent europium ions Eu^{2+} are widespread activators for inorganic luminescent materials. In recent years, Eu^{2+} was considered as a promising dopant for scintillator applications due to a high light yield of doped single crystals. In this paper, we studied the luminescent properties of Eu^{2+} doped $LaCl_3$ microcrystals embedded in the NaCl matrix $LaCl_3$:Eu^{2+} microcrystals dispersed in the NaCl matrix have been obtained in the NaCl–$LaCl_3$(1 mol.%)– $EuCl_3$(0.1 mol.%) crystalline system. The low-temperature luminescent properties of these microcrystals have been studied upon the VUV and UV excitation by the synchrotron radiation. The spectroscopic parameters as well as decay time constants of Eu^{2+} doped $LaCl_3$ host have been established. The excitation mechanism of divalent europium centers through energy transfer and reabsorption is discussed.

B. Kinetics of processes with self-organization

DYNAMIC SELF-ASSEMBLY OF PHOTO-SWITCHABLE NANOPARTICLES

V.N. Kuzovkov,
Prateek K. Jha, B. Grzybowski and M. Olvera de la Cruz (*Northwestern University, Evanston, USA*)

Nanoparticles functionalized with photo-switchable ligands can be assembled into a broad range of structures by controlled light exposure. In particular, alternating light exposures provide the means to control formation of assemblies of various sizes and symmetries. Here, *in collaboration with Northwestern University, Evanston, USA,* we use scaling arguments and Kinetic Monte Carlo simulations to study the evolution of reversible aggregates in a solution of periodically irradiated photo-switchable nanoparticles. Scaling estimates of the characteristic size and the mean separation of aggregates agree with the simulations. The transition probabilities in the Kinetic Monte Carlo scheme are derived from a renormalized master equation of the diffusion process. Simulations on a system of nanoparticles, interacting through Lennard-Jones pair potentials that change their character from repulsive to attractive depending on the light exposure, show that the slow diffusion of particles at low effective temperatures (where the attractions are much higher than the thermal energy) results in the formation of small, ‘‘kinetically frozen’’ aggregates. On the other hand, aggregation does not occur at high effective temperatures, where the attractions are comparable to the thermal energy. In the intermediate range of effective temperatures,

‘‘fluctuating’’ aggregates form that can be stabilized by applying light pulses of specific lengths and frequencies. The aggregate sizes increase by increasing the packing fraction and the aggregates undergo transition to a percolated ‘‘network’’ at high packing fractions. Light-control of inter-particle interactions can either inhibit or promote nucleation and growth, and can reduce gel and glass formation.

THE KINETIC MONTE CARLO SIMULATIONS OF FLOW-ASSISTED POLYMERIZATION

V.N. Kuzovkov,
Prateek K. Jha and M. Olvera de la Cruz (*Northwestern University, Evanston, USA*)

In collaboration with Northwestern University, Evanston, USA, we performed kinetic Monte Carlo simulations on a model of a polymerization process in the presence of a periodic oscillatory flow to explore the role of mixing in polymerization reactors. Application of an oscillatory flow field helps overcome the diffusive limitations that develop during a polymerization process due to an increase in the molecular weights of polymer chains, thereby giving rise to high rates of polymerization. A systematic increase in the flow strength results in a “dynamic” coil−stretch transition, leading to an elongation of polymer chains. Reactive ends of stretched (polymer) chains react more frequently than the reactive ends of coiled chains, which are screened by other monomers of the same chain. There exists a critical flow strength for the efficiency of polymerization processes. The kinetic Monte Carlo simulation scheme developed here exhibit great promise for the study of dynamic properties of polymer systems.

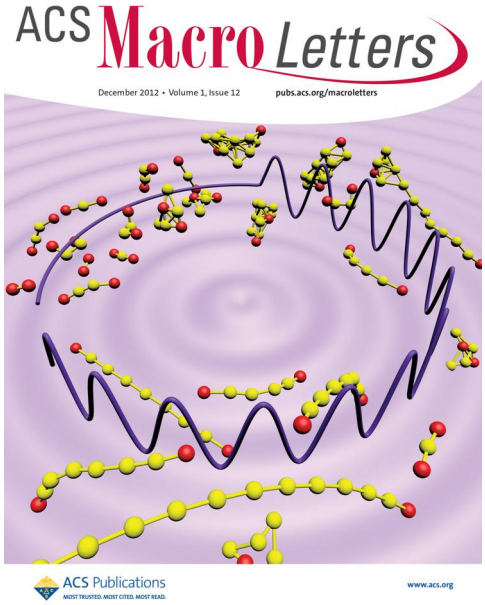

Fig.16. Cover page of the ACS Macro Letters with the presentation of this paper.

STATISTICAL ANALYSIS AND CELLULAR AUTOMATA MODELING OF VOID LATTICE FORMATION IN ELECTRON IRRADIATED CaF_2

P Merzlyakov, G Zvejnieks, V N Kuzovkov and E A Kotomin

Calcium fluoride (CaF_2) is widely used in both microlithography and as a deep UV window material. It is also known that electron beam irradiation creates a *superlattice* consisting of periodically distributed fluorine vacancy clusters (called a *void lattice*).

To perform a quantitative analysis of experimental TEM image data demonstrating void lattice formation under electron irradiation of CaF_2, we developed two distinct image filters. As a result, we can easily calculate vacancy concentration, cluster distribution function as well as average distance between clusters. In particular, an analysis of the consecutive experimental snapshots obtained by increasing irradiation dose, allows us to restore the void lattice formation process. The results for two suggested filters are similar and demonstrate that void cluster growth is accompanied with a slight increase of the superlattice parameter.

Despite numerous experiments, the void superlatticelattice formation in CaF_2 under electron irradiation still possesses open questions regarding the microscopic processes that govern the self-organization phenomenon. We propose a microscopic model that allows us to reproduce a macroscopic ordering in a form of void lattice, in agreement with experimental data and provide an explanation for existing theoretical and experimental contradictions. We consider fluorine sublattice, where irradiation produces correlated Frenkel defects – pairs of the F and H centers. Slow F center diffusion is accompanied with their nearest neighboring attractive interaction leading to the formation of F center clusters, i.e., voids. The driving forces for the long-range void ordering are H center planes. They are formed by highly mobile H centers due to three-atoms-in-a-line (trio) attractive interactions, see Fig. 17.

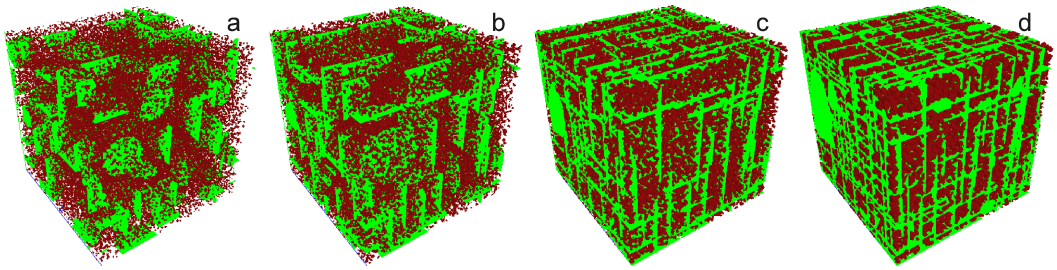

Fig. 17. 3D CA simulation snapshots at the following dimensionless F center 3D concentrations and CA simulation times (a) (0.02, 0.025 s), (b) (0.04, 0.057 s), (c) (0.10, 0.207 s), (d) (0.17, 0.542 s). The F centers are marked red, the H centers - light green.

Our cellular automata simulations demonstrate that global void lattice self-organization can occur only in a narrow parameter range where an average spacing between void clusters

and H center planes is balanced. Moreover, we monitor also the kinetics of a void lattice ordering starting from an initial disordered stage, in agreement with the TEM experimental data.

C. Plasma Physics

BIFURCATION ANALYSIS IN A 3D SYSTEM MODELING OSCILLATING PHENOMENA IN FUSION PLASMA PHYSICS

O. Dumbrajs,
D. Constantinescu,
Dept of Applied Mathematics, University of Craiova, Romania
V. Igochine, K. Lackner, H. Zohm
Max-Planck Institut für Plasmaphysik, Garching, Germany

The aim of this paper was a study of a 3D dynamical system which models some instabilities that occur in fusion plasma experiments in TOKAMAKs (toroidal devices for obtaining energy through controlled thermonuclear fusion). This model depends on three parameters. It was formulated for the description of a system with drive and relaxation processes which have different time scales. It has some properties analogue to Lorenz system, but it does not belong to the family of Lorenz-like systems. We systematically study the dynamics of the system for various values of the parameters and we provide analytical results concerning some bifurcations that occur in the parameters space. We theoretically analyze the fast-slow dynamics of the system and we apply the results in some situations which correspond to experimental data obtained in ASDEX-Upgrade tokamak.

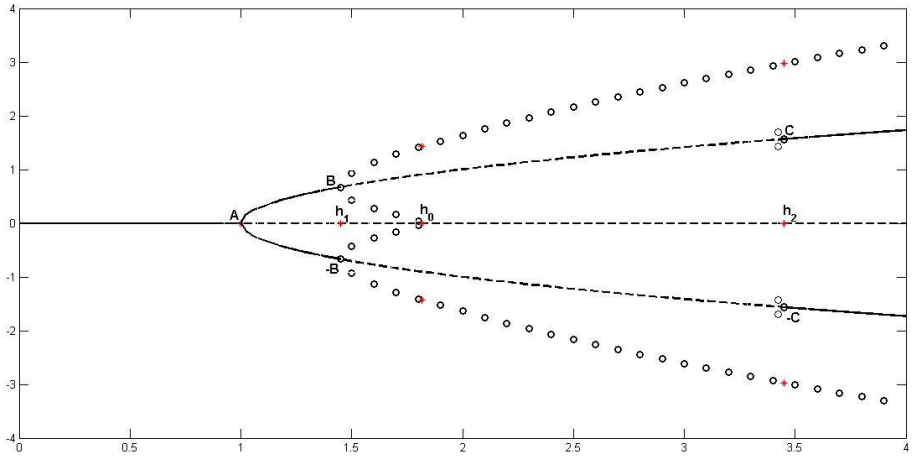

Fig.18. Bifurcation diagram for a fixed values of δ=0.2, η=0.2, pitchfork bifurcation (labelled A) in h=1, two pairs of Hopf bifurcations (labelled B, -B respectively C, -C) in h_1 and h_2, homoclinic bifurcation in h_0.

ANALYSIS OF AFTERCAVITY INTERACTION IN EUROPEAN ITER GYROTRONS AND IN THE COMPACT SUB-THZ GYROTRON FU CW-CI

O. Dumbrajs
T. Idehara
Research Center for Development of FI Region, University of Fukui (FIR FU), Japan

Possibilities of arising of aftercavity interaction are analyzed in the ITER 170 GHz 2 MW coaxial cavity gyrotron and the 170 GHz 1 MW cylindrical cavity gyrotron, as well as in the compact 394.5 GHz low power gyrotron FU CW-CI. Also, the simulations for the gyrotron efficiency in the presence of aftercavity interaction are performed in the cold cavity approximation. Results of the analysis illustrate the subtle interplay between the geometry of the output taper and the profile of the magnetic field.

REGIONS OF AZIMUTHAL INSTABILITY IN GYROTRONS

O. Dumbrajs,
G. S, Nusinovich, and T. M. Antonsen, Jr.
Institute for Research in Electronics and Applied Physics, University of Maryland, USA

This paper is devoted to the analysis of the instability of operating modes in high-power gyrotrons with cylindrically symmetric resonators. This instability manifests itself in destruction of the azimuthally uniform wave envelope rotating in a gyrotron resonator having a transverse size greatly exceeding the wavelength. The appearance of azimuthally nonuniform solutions can be interpreted as simultaneous excitation of modes with different azimuthal indices. This problem is studied self-consistently, i.e. taking into account the temporal evolution of both the azimuthal and axial structures of the wave envelope. The region of gyrotron operation free from this instability is identified. The efficiency achievable in this region can be only 1-2% lower than the maximum efficiency. It is also possible to address the difference between the theory of mode interaction developed under assumption that all modes have fixed axial structure and the self-consistent theory presented here. As known, for fixed axial mode profiles, single-mode high-efficiency oscillations remain stable no matter how dense is the spectrum of competing modes, while the self-consistent theory predicts stable high-efficiency operation only when the azimuthal index does not exceed a certain critical value. It is shown that the azimuthal instability found in the self-consistent theory is caused by excitation of modes having axial structures different from that of the desired central mode.

Defence of PhD Theses

The Doctoral Thesis D. Bocharov “First principles simulations on surface properties and reactivity of sustainable nitride nuclear fuels” was defended in January 2012 at the University of Latvia.

Publications in year 2012

SCI

1. P. Savchyn, I. Karbovnyk, V. Vistovskyy, A. Voloshinovskii, V. Pankratov, M. Cestelli Guidi, C. Mirri, O. Myahkota, A. Riabtseva, N. Mitina, A. Zaichenko, and **A.I. Popov**, Vibrational properties of $LaPO_4$ nanoparticles in mid- and far-infrared domain. - J. Appl. Phys., 2012, **112**, 124309 (p. 1-6).

2. **R.I. Eglitis**, *Ab initio* calculations of the atomic and electronic structure of $SrZrO_3$ (111) surfaces. - Ferroelectrics, 2012, **436**, p. 5-11.

3. **Yu.F. Zhukovskii**, **S. Piskunov**, and S. Bellucci, Double-wall carbon nanotubes of different morphology: electronic structure simulations. - Nanosci. Nanotechnol. Lett., 2012, **4**, p. 1074-1081.

4. P.K. Jha, **V.N. Kuzovkov**, and M. Olvera de la Cruz, Kinetic Monte Carlo simulations of flow-assisted polymerization. - ACS Macro Lett., 2012, **1**, p. 1393−1397.

5. **O. Dumbrajs**, T. Idehara, T. Saito, and Y. Tatematsu, Calculations of starting currents and frequencies in frequency-tunable gyrotrons. - Jpn. J. Appl. Phys., 2012, **51**, 126601 (p. 1-5).

6. **O. Dumbrajs** and G.S. Nusinovich, On optimization of sub-THz gyrotron parameters. - Phys. Plasmas, 2012, **19**, 103112 (p. 1-6).

7. **O. Dumbrajs** and T. Idehara, Analysis of aftercavity interaction in European ITER gyrotrons and in the compact Sub-THz gyrotron FU CW-CI. - J. Infrared Milli. Terahz. Waves, 2012, **33**, p. 1171–1181.

8. J.R. Kalnin and **E.A. Kotomin**, Note: Effective diffusion coefficient in heterogeneous media. - J. Chem. Phys., 2012, **137**, 166101 (p. 1-2).

9. **Yu.N. Shunin**, **Yu.F. Zhukovskii**, V.I. Gopeyenko, N. Burlutskaya, T. Lobanova-Shunina, and S. Bellucci, Simulation of electromagnetic properties in carbon nanotubes and graphene-based nanostructures. - J. Nanophotonics, 2012, **6**, 061706 (p. 1-16).

10. **A. Sorokine**, **D. Bocharov**, **S. Piskunov**, and **V. Kashcheyevs**, Electronic charge redistribution in $LaAlO_3$(001) thin films deposited at $SrTiO_3$(001) substrate: First-principles analysis and the role of stoichiometry. - Phys. Rev. B, 2012, **86**, 155410 (p. 1-10).

11. M.M. Kuklja, **Yu.A. Mastrikov**, B. Jansang, and **E.A. Kotomin**, The Intrinsic Defects, Disordering, and Structural Stability of $Ba_xSr_{1-x}Co_yFe_{1-y}O_{3-\delta}$ Perovskite Solid Solutions. - J. Phys. Chem. C, 2012, **116**, p. 18605-18611.

12. A.F Fix, F.U. Abuova, **R.I. Eglitis**, **E.A. Kotomin**, and A.T. Akilbekov, *Ab initio* calculations of the *F* centers in MgF_2 bulk and on the (001) surface. - Phys. Scr., 2012, **86**, 035304 (p. 1-5).

13. L. Wang, R. Merkle, **Yu.A. Mastrikov**, **E.A. Kotomin**, and J. Maier, Oxygen exchange kinetics on solid oxide fuel cell cathode materials—general trends and their mechanistic interpretation. - J. Mater. Res., 2012, **27**, p. 2000-2008.

14. A. Reinfelds, **O. Dumbrajs**, H. Kalis, J. Cepitis, and D. Constantinescu, Numerical experiments with single mode gyrotron equations. - Math. Model. Anal., 2012, **17**, p. 251–270.

15. J. Cepitis, **O. Dumbrajs**, H. Kalis, A. Reinfelds, and U. Strautins, Analysis of equations arising in gyrotron theory. - Nonlinear Analysis: Modelling and Control, 2012, **17**, p. 139–152.

16. **O. Dumbrajs**, G.S. Nusinovich, and T.M. Antonsen, Regions of azimuthal instability in gyrotrons. - Phys. Plasmas, 2012, **19**, 063103 (p. 1-7).

17. **Yu.F. Zhukovskii** and R.A. Evarestov, *Ab initio* simulations on rutile-based titania nanowires. - IOP Conf. Series: Mater. Sci. Engineering, 2012, **38**, 012005 (p. 1-6).

18. **A.V. Sorokin**, **Yu.F. Zhukovskii**, J. Purans, and **E.A. Kotomin**, The effect of Zn vacancies and Ga dopants on the electronic structure of ZnO: *Ab initio* simulations. - IOP Conf. Series: Mater. Sci. Engineering, 2012, **38**, 012015 (p. 1-4).

19. F.U. Abuova, A.T. Akilbekov, and **E.A. Kotomin**, *Ab initio* calculations of the H centers in MgF_2 crystals. - IOP Conf. Series: Mater. Sci. Engineering, 2012, **38**, 012041 (p. 1-4).

20. **O. Lisovski**, **S. Piskunov**, **Yu.F. Zhukovskii**, and J. Ozolins, *Ab initio* modeling of sulphur doped TiO_2 nanotubular photocatalyst for water-splitting hydrogen generation. - IOP Conf. Series: Mater. Sci. Engineering, 2012, **38**, 012057 (p. 1-5).

21. **E.A. Kotomin**, **Yu.F. Zhukovskii**, **D. Bocharov**, and **D. Gryaznov**, *Ab initio* modelling of UN grain boundary interfaces. - IOP Conf. Series: Mater. Sci. Engineering, 2012, **38**, 012058 (p. 1-4).

22. R.A. Evarestov, D.B. Migas, and **Yu.F. Zhukovskii**, Symmetry and stability of the rutile-based TiO_2 nanowires: models and comparative LCAO-plane wave DFT calculations. - J. Phys. Chem. C, 2012, **116**, p. 13395–13402.

23. **Yu.F. Zhukovskii**, **E.A. Kotomin**, **S. Piskunov**, and S. Bellucci, CNT arrays grown upon catalytic nickel particles as applied in the nanoelectronic devices: *Ab initio* simulation of growth mechanism. - Proc. NATO ARW „Nanodevices and Nanomaterials for Ecological Security" (Eds. **Yuri N. Shunin** and Arnold E. Kiv; Springer: Dordrecht, 2012), p. 101-114.

24. **R.I. Eglitis**, *Ab initio* calculations of $SrTiO_3$(111) surfaces. - Proc. NATO ARW „Nanodevices and Nanomaterials for Ecological Security" (Eds. **Yuri N. Shunin** and Arnold E. Kiv; Springer: Dordrecht, 2012), p. 125-132.

25. **A. Gopejenko**, **Yu.F. Zhukovskii**, P.V. Vladimirov, **E.A. Kotomin**, and A. Möslang, Interaction between oxygen and yttrium impurity atoms as well as vacancies in *fcc* iron lattice: *Ab initio* modeling. - Proc. NATO ARW „Nanodevices and Nanomaterials for Ecological Security" (Eds. **Yuri N. Shunin** and Arnold E. Kiv; Springer: Dordrecht, 2012), p. 149-160.

26. **Yu.N. Shunin**, **Yu.F. Zhukovskii**, N. Burlutskaya, V.I. Gopeyenko, and S. Bellucci, Simulation of fundamental properties of CNT- and GNR-metal interconnects for development of new nanosensor systems. - Proc. NATO ARW „Nanodevices and Nanomaterials for Ecological Security" (Eds. **Yuri N. Shunin** and Arnold E. Kiv; Springer: Dordrecht, 2012), p. 237-262.

27. R.A. Evarestov, E. Blokhin, **D. Gryaznov**, **E.A. Kotomin**, R. Merkle, and J. Maier, Jahn-Teller effect in the phonon properties of defective $SrTiO_3$ from first principles. - Phys. Rev. B, 2012, **85**, 175303 (p.1-5).

28. **Yu.N. Shunin**, **Yu.F. Zhukovskii**, N. Burlutskaya, and S. Bellucci, CNT-metal interconnects: Electronic structure calculations and resistivity simulations. - J. Nanoelectronics & Optoelectronics, 2012, **7**, N 1, p. 3–11.

29. **D. Gryaznov**, E. Heifets, and **E.A. Kotomin**, The first-principles treatment of the electron-correlation and spin–orbital effects in uranium mononitride nuclear fuels. - Phys. Chem. Chem. Phys., 2012, **14**, p. 4482–4490.

30. H. Shi, L. Chang, R. Jia, and **R.I. Eglitis**, Ab initio calculations of hydroxyl impurities in CaF_2. - J. Phys. Chem. C, 2012, **116**, p. 6392-6400.

31. H. Shi, L. Chang, R. Jia, and **R.I. Eglitis**, Ab initio calculations of the transfer and aggregation of *F* centers in CaF_2. - J. Phys. Chem. C, 2012, **116**, p. 4832-4839.

32. E. Blokhin, **E.A. Kotomin**, and J. Maier, First-principles phonon calculations of Fe^{4+} impurity in $SrTiO_3$. - J. Phys.: Condens. Matter, 2012, **24** 104024 (p. 1-4).

33. R. Merkle, **Yu.A. Mastrikov**, **E.A. Kotomin**, M.M. Kuklja, and J. Maier, First principles calculations of oxygen vacancy formation and migration in $Ba_{1-x}Sr_xCo_{1-y}Fe_yO_{3-\delta}$ perovskites. - J. Electrochem. Soc., 2012, **159**, p. B219-B226.

34. P.V. Savchyn, V.V. Vistovskyy, A.S. Pushak, A.S. Voloshinovskii, A.V. Gektin, V. Pankratov, and **A.I. Popov**, Synchrotron radiation studies on luminescence of Eu^{2+}-doped $LaCl_3$ microcrystals embedded in a NaCl matrix. - Nucl. Instr. Meth. Phys. Res. B, 2012, **274**, p. 78-82.

35. P.K. Jha, **V.N. Kuzovkov**, B.A. Grzybowski, and M. Olvera de la Cruz, Dynamic self-assembly of photo-switchable nanoparticles. - Soft Matter, 2012, **8**, p. 227–234.

Chapters in Scientific Books

Yu.F. Zhukovskii, **D. Bocharov**, **D. Gryaznov**, and **E.A. Kotomin**, First Principles Simulations on Surface Properties and Oxidation of Nitride Nuclear Fuels. - Chapter in a book: Advances in Nuclear Fuel (Ed. Shripad T. Revankar, InTech Open Acess Publishers), 2012, p. 95-122.

Presentations at scientific conferences, congresses, meetings, schools and workshops

I. I. 28th ISSP Conference (Riga, Latvia, February, 2012).

1. D. Constantinescu, O. Dumbrajs, V. Igochine, K. Lackner, R. Meyer-Spasche, H. Zohm, and ASDEX Upgrade team, "A low-dimensional model system for quasi-periodic plasma perturbations". Abstracts: p. 5.

2. O. Lisovski, S. Piskunov, Yu.F. Zhukovskii, and J. Ozolins, „Quantum-chemical simulations of TiO_2 nanotubes for photocatalytic hydrogen generation." Abstracts: p. 7.

3. D. Bocharov, Yu.F. Zhukovskii, D. Gryaznov, and E.A. Kotomin, "Surface modeling of UN and other actinides: Current state and prospects". Abstracts: p. 16.

4. R.I. Eglitis, H. Shi, R. Jia, L. Yue, and X. He, "Ab initio calculations for the H centers in SrF_2 as well as surface H centers and F centers aggregation in BaF_2". Abstracts: p. 17.

5. A.V. Sorokin, Yu.F. Zhukovskii, D. Gryaznov, J. Purans, and E.A. Kotomin, "Influence of the concentration of zinc vacancies on electronic properties of ZnO". Abstracts: p. 18.

6. A. Gopejenko, Yu.F. Zhukovskii, P.N. Vladimirov, E.A. Kotomin, Yu.A. Mastrikov, and A. Möslang. "Ab initio calculations of binding energies between defects in fcc Fe lattice for further kinetic Monte-Carlo simulation on ODS steel". Abstracts: p. 19.

7. P. Zhgun, A. Kuzmin, D. Bocharov, and S. Piskunov, " Ab intio calculations on the structure of SF_3". Abstracts: p. 22.

8. L. Shirmane, V. Pankratov, A.I. Popov, A. Kotlov, P. Gluchowski, and W. Strek, "Luminescence of $MgAl_2O_4:Cr^{3+}$ nanocrystals under synchrotron radiation". Abstracts: p. 77.

II. APS March Meeting 2012 (Boston, USA, February-March, 2012).

9. P. Jha, V.N. Kuzovkov, B. Grzybowski, and M. Olvera de la Cruz, "A novel Kinetic Monte Carlo algorithm for non-equilibrium simulations". Abstracts: D52.00005.

III. IMEC-15, The 15th Israel Materials Engineering Conference, (Dead Sea, Israel, February-March, 2012).

10. A. Weizman, D. Fuks, D. Gryaznov, and E.A. Kotomin, Ab initio study of phase equilibria in $(La_x,Sr_{1-x})CoO_3$ solid solutions.

IV. 10th International Conference "Information Technologies and Management", IT&M'2012 (Riga, Latvia, April, 2012).

11. Yu.N. Shunin, „Novel carbon-based nanosensors". Abstracts: p. 15-16.

12. Yu.F Zhukovskii and R.A. Evarestov, "Symmetry analysis and first-principles calculations on rutile-based titania [001] and [110] nanowires". Abstracts: p. 17-18.

13. A. Gopejenko, Yu.F. Zhukovskii, P.V. Vladimirov, E.A. Kotomin, and A. Möslang, "Quantum chemical calculations of binding energies between Y and O impurity atoms and Fe vacancies inside iron lattice for ODS steels". Abstracts: p. 19.

14. Yu.N. Shunin, Yu.F. Zhukovskii, V.I. Gopeyenko, N. Burlutskaya, and S. Bellucci, "Simulation of electromagnetic properties in carbon-based nanointerconnects". Abstracts: p. 21.

15. S. Piskunov and E. Spohr, "$SrTiO_3$ nanotubes with negative strain energy predced from first principles". Abstracts: p. 22.

16. O. Lisovski, S. Piskunov, Yu.F. Zhukovskii, and J. Ozolins, "Quantum chemical simulations of doped TiO_2 nanotbes for photocatalyic hydrogen generation". Abstracts: p. 23

17. Yu.N. Shunin, V.I Gopeyenko, P.N Dyachkov, N. Burlutskaya, Yu.F. Zhukovskii, and S. Bellucci, "Simulation of CNT conductivity for various nanotube chiralities". Abstracts: p. 24.

V. 8th International Conference "Functional Materials and Nanotechnologies" FM&NT-2012 (Riga, Latvia, April, 2012).

18. R.I. Eglitis, H. Shi, R. Jia, L. Yue, and X. He, Ab initio calculations for the H centers in SrF_2 as well as surface H centers in BaF_2 and F centers aggregation in BaF_2 and CaF_2. – Abstract: p. 63.

19. D. Gryaznov, R.A. Evarestov, E. Blokhin, E.A. Kotomin, and J. Maier, Ab initio thermodynamic calculations of oxygen vacancies in perovskites: the case study of $(La,Sr)(Co,Fe)O_{3-\delta}$ and $SrTiO_{3-\delta}$ – Abstract: p. 67.

20. J.R. Kalnin and E.A. Kotomin, One-dimensional diffusion in heterogeneous medium. – Abstract: p. 68.

21. E.A. Kotomin, Yu.A. Mastrikov, J. Maier, M.M. Kuklja, A. Weizman, and D. Fuks, First principles calculations of structural stability for complex perovskites. – Abstract: p. 71.

22. Yu.A. Mastrikov, D. Gryaznov, E.A. Kotomin, R. Merkle, M.M. Kuklja, and J. Maier, First principles study of oxygen vacancies in perovskite solid solutions. – Abstract: p. 81.

23. Yu.N. Shunin, Yu.F. Zhukovskii, V.I. Gopeyenko, N. Burlutskaya, and S. Bellucci, Electromagnetic properties of CNT and graphene-based nanostructures. – Abstract: p. 90.

24. R.A. Evarestov and Yu.F. Zhukovskii, First principles calculations on properties of the rutile-based TiO_2 nanowires with Ti-atom centered symmetry axes. – Abstract: p. 98.

25. G. Zvejnieks, V.N. Kuzovkov, E.A. Kotomin, and M.O. de la Cruz, Microscopic approach to the kinetics of pattern formation of charged molecules on surfaces. – Abstract: p. 99.

26. E. Blokhin, D. Gryaznov, R.A. Evarestov, and J. Maier, A new approach to the engineering of ab initio materials simulations on an example of CRYSTAL, VASP and WIEN2k packages.– Abstract: p. 115.

27. E. Blokhin, A. Kuzmin, J. Purans, E.A. Kotomin, R.A. Evarestov, and J. Maier, Joint theoretical-experimental study of iron impurities and oxygen vacancies in $SrTiO_3$. – Abstract: p. 116.

28. E. Klotins and G. Zvejnieks, Treatment of excitons by discrete variable representation. – Abstract: p. 118.

29. R.I. Eglitis, Ab initio calculations of $SrTiO_3$, $BaTiO_3$, $PbTiO_3$, $CaTiO_3$, $BaZrO_3$, $SrTiO_3$, as well as $PbTiO_3$ (001),(011) and (111) surfaces including Nb impurity segregation towards the $SrTiO_3$ surface.– Abstract: p. 124.

30. P. Zhgun, D. Bocharov, S. Piskunov, A. Kuzmin, and J. Purans, Electronic structure and lattice dynamics of ScF_3 from ab initio LCAO calculations.– Abstract: p. 125.

31. A. Sorokin, D. Gryaznov, Yu.F. Zhukovskii, E.A. Kotomin, and J. Purans, First principles calculations of defective ZnO crystals: the role of symmetry and phonons.– Abstract: p. 126.

32. A. Usseinov, A. Sorokin, Yu.F. Zhukovskii, E.A. Kotomin, A.T. Alikbekov, and J. Purans, Ab initio calculations of hydrogen impurities in ZnO.– Abstract: p. 127.

33. L. Shirmane, A. Kuzmin, A.I. Popov, and V. Pankratov, Raman scattering study of $YVO_4:Eu^{3+}$ nanocrystals.– Abstract: p. 215.

34. I. Bolesta, I. Karbovnyk, I. Rovetsky, S. Velgosh, I. Kityk, V. Pankratov, and A.I. Popov, Effect of aging on the luminescence of pure and dopped CdI_2.– Abstract: p. 220.

35. A.I. Popov, V. Pankratov, E. Klotins, L. Shirmane, V. Dimza, M. Antonova, M. Livinsh, and A. Kotlov, VUV synchrotron radiation spectroscopy of PLZT ceramics.– Abstract: p. 221.

36. A. Kuzmin, V. Pankratov, A. Kalinko, A. Kotov, L. Shirmane, and A.I. Popov, Electronic excitation in $NiWO_4$ using VUV synchrotron radiation. – Abstract: p. 230.

37. O. Lisovski, S. Piskunov, Yu.F. Zhukovskii, and J. Ozolins, Quantum chemical simulations of doped TiO_2 nanotubes for photocatalytic hydrogen generation.– Abstract: p. 275.

38. J. Kazerovskis, S. Piskunov, Yu.F. Zhukovskii, P.N. Dyachkov, S. Belucci, and M. Utinans, Atomic electronic properties and of Ni filament encapsulated inside single-walled carbon nanotubes of different chiralities.– Abstract: p. 276.

39. J. Begens, S. Piskunov, Yu.F. Zhukovskii, E. Spohr, and M. Utinans, Quantum chemical simulations of doped $SrTiO_3$ nanotubes for application in photocatalytic reactions.– Abstract: p. 277.

40. Yu.N. Shunin, V.I. Gopeyenko, P.N. Dyachkov, N. Burlutskaya, Yu.F. Zhukovskii, and S. Bellucci, Parametric simulation of CNT dc- and ac-conductivity for various nanotibe chiralities. - Abstract: p.278.

41. P. Nazarov and V. Kashcheyevs, Finite temperature effects in single-parameter non-adiabatic electron pumps.– Abstract: p. 280.

42. J. Timoshenko and V. Kashcheyevs, Modeling of non-adiabatic quantum pumps.– Abstract: p. 281.

43. P. Merzlakov, G. Zvejnieks, V.N. Kuzovkov, E.A. Kotomin, K.D. Li, and L.M. Wang, Analysis of void superlattice formation in CaF_2.– Abstract: p. 282.

44. G. Zvejnieks, V.N. Kuzovkov, and E.A. Kotomin, Atomistic theory of messcopc pattern formation induced by bimolecular surface reactions between oppositely charged molecules. – Abstract: p. 283.

45. V.N. Kuzovkov, E.A. Kotomin, and M.O. de la Cruz, The non-equilibrium charge screening effects in diffusion-driven systems. – Abstract: p. 285.

46. V.N. Kuzovkov, The Anderson localization problem, the Fermi-Pasta-Ulam paradox and the generalized diffusion approach.– Abstract: p. 286.

47. P. Jha, V.N. Kuzovkov, B. Grzybowski, and M.O. de la Cruz, Light induced self-assembly of switchable colloids. – Abstract: p. 285.

48. D. Bocharov, Yu.F. Zhukovskii, D. Gryaznov, and E.A. Kotomin, Ab initio modeling of uranium nitride grain boundary interfaces. – Abstract: p. 304.

49. F.U. Abuova, A.F. Fix, A.T. Akilbekov, S. Piskunov, E.A. Kotomin, and R.I. Eglitis, Ab initio calculations of bulk and surface defects in MgF_2 crystals. – Abstract: p. 305.

50. A. Gopejenko, Yu.F. Zhukovskii, P.V. Vladimirov, E.A. Kotomin, and A. Möslang, Quantum chemical simulations on binding energies of pair and tripe-wise defects in fcc-Fe lattice for ODS steels. – Abstract: p. 306.

VI. 13th International V.A. Fock Meeting on Quantum and Computational Chemistry (Astana, Kazakhstan, April, 2012)

51. R.A. Evarestov and Yu.F. Zhukovskii, Symmetry and properties of the rutile-based titania nanowires. – Abstract: p. 28.

52. F.U. Abuova, A.F. Fix, A.T. Akilbekov, E.A. Kotomin, and R.I. Eglitis, Ab initio calculations of bulk and surface color centers in MgF_2 crystals. – Abstract: p. 48.

53. Yu.F. Zhukovskii, D. Bocharov, D. Gryaznov and E.A.Kotomin, First-principles simulations on surface properties and oxidation of uranium mononitrde. – Abstract: p. 53.

VII. 5th International Conference on Innovative Information Technologies, IIT-2012 (Vilnius, Lithuania, May, 2012).

54. Yu.N. Shunin, T. Lobanova-Shunina, N. Burlutskaya, and S. Bellucci, Novel carbon-based nanosensors for living and artificial complex systems. - Abstracts: p. 6.

55. Yu.N. Shunin, V.I. Gopeyenko, P.N. Dyachkov, N. Burlutskaya, Yu.F. Zhukovskii, and S. Bellucci, Simulation of dc- and ac-conductivity for armchair carbon nanotubes. - Abstracts: p. 7.

VIII. Spring European Materials Research Society (E-MRS) Meeting (Strasbourg, France, May, 2012).

56. Yu.A. Mastrikov, E.A. Kotomin, R. Merkle, M.M. Kuklja, and J. Maier, First principles calculations of formation and migration of oxygen vacancies in $La_{1-x}Sr_xCo_{1-y}Fe_yO_{3-\delta}$ perovskites. – Abstract: C7-2.

57. M.M. Kuklja, Yu.A. Mastrikov, B. Jansang, and E.A. Kotomin, First principles calculations of $(Ba,Sr)(Co,Fe)O_3$ structural stability. – Abstract: C7-3.

58. A. Weizman, D. Fuks, D. Gryaznov, and E.A. Kotomin, Ab initio study of phase competition in $(La_x,Sr_{1-x})CoO_3$. – Abstract CP5-8.

59. R.I. Eglitis, Ab initio calculations of $SrTiO_3$, $BaTiO_3$, $PbTiO_3$, $CaTiO_3$, $BaZrO_3$, $SrZrO_3$ and $PbZrO_3$ (001), (011) and (111) surfaces as well as Nb impurity segregation towards the $SrTiO_3$ surface. – Abstract: CP12-1.

60. D. Gryaznov, D. Fuks, and J. Maier, Ab initio thermodynamic calculations on $(La,Sr)(Co,Fe)O_3$ solid solutions. – Abstract: CP12-2.

61. D. Gryaznov, E. Heifets, and E.A. Kotomin, The first-principles treatment of the electron-correlation and spin-orbital effects in uranium mononitride nuclear fuels. – Abstract: E1-4.

62. E.A. Kotomin, D. Gryaznov, D. Bocharov, and Yu.F. Zhukovskii, Ab initio simulations of oxygen adsorption and migration upon uranium nitride surfaces. – Abstract: E2-2.

63. R.I. Eglitis, Ab initio calculations of $SrZrO_3$ and $PbZrO_3$ (001) and (011) surfaces as well as F center on ZrO_2-terminated $PbZrO_3$ (001) surface. – Abstract: L8P-17.

64. R.I. Eglitis, H. Shi, R. Jia, L. Yue, and X. He, Ab initio calculations for the H centers in SrF_2 as well as surface H centers and F centers aggregation in BaF_2. – Abstract: VO-3.

IX. International Conference on Fundamental and Applied NanoElectroMagnetics, FANEM'12 (Minsk, Belarus, May, 2012)

65. Yu.N. Shunin, Yu.F. Zhukovskii, N. Burlutskaya, T. Lobanova-Shunina, V.I. Gopeyenko, and S. Bellucci. Simulation of electromagnetic properties in CNT- and graphene-based nanostructures. - Abstract: p. 9.

X. 17th Joint workshop on electron cyclotron emission and electron cyclotron resonance heating (Deurne, The Netherlands, May, 2012).

66. K.A. Avramides, A.K. Ram, O. Dumbrajs, S. Alberti, T.M. Tran, and S. Kern, On the numerical scheme employed in gyrotron interaction simulations.

XI. 17th International Conference on Mathematical Modelling and Analysis (MMA2012), (Tallinn, Estonia, June, 2012).

67. O. Dumbrajs and A. Reinfelds, Qualitative investigation of dynamical system arising in plazma physics.

XII. Annual Monitory Meeting of European Fusion Development Agreement, EFDA - 2012 (Ljubljana, Slovenia, June, 2012).

68. Yu.A. Mastrikov, P.V. Vladimirov, V.A. Borodin, Yu.F. Zhukovskii, E.A. Kotomin, and A. Möslang, Ab initio simulation of growth of vacancies formed clusters in α-Fe lattice.

XIII. The 17th International Conference on Defects in Insulating Materials, ICDIM'12 (Santa Fe, Arizona, USA, June, 2012).

69. E.A. Kotomin, R. Merkle, Yu.A. Mastrikov, M. Kuklja, D. Fuks, and J. Maier, First principles calculations on defects in ABO_3 perovskites: Applications for oxygen permeation membranes and SOFC cathodes. - Abstract: p.18.

70. F.U. Abuova, A.K. Dauletbekova, A.T. Akilbekov, E.A. Kotomin, and Zh.K. Yermekova, First principles calculations on radiation defects in MgF_2 crystals. - Abstract: p. 110.

XIV. "Nature Materials", Frontiers in Electronic Materials: Correlation Effects and Memristive Phenomena (Aachen, Germany, June, 2012).

71. R. Merkle, L. Wang, Y. A. Mastrikov, E. A. Kotomin, and J. Maier, Oxigen exchange kinetics on perovskite surfaces: importance of electronic and ionic defects.

XV. 10th international conference on Solid State Chemistry (Pardubice, Czech Republic, June, 2012).

72. R. Merkle, L.Wang, Yu.A. Mastrikov, A. Wedig, E.A. Kotomin, and J. Maier, Mechanistic insight into oxygen exchange SURFACE reaction on perovskites from experiments and DFT calculations.

XVI. 10th International Symposium on Systems with fast ionic transport (ISSFIT) (Chernogolovka, Russia, July, 2012).

73. E.A. Kotomin, R. Merkle, Yu.A. Mastrikov, M. Kuklja, D. Fuks, and J. Maier, Ab initio modelling of oxygen transport in mixed conducting perovskites. - Abstract: p.14.

XVII. International Workshop on Nanocarbon Photonics and Optoelectronics, NPO-2012 (Huhmari-Polvijärvi, Finland, July-August, 2012).

74. Yu.N. Shunin, Yu.F. Zhukovskii, V.I. Gopeyenko, N. Burlutskaya, T. Lobanova-Shunina, and S. Bellucci, Electromagnetic properties in carbon- and graphene-based monoperiodic nanostructures for nanosensor systems.

XVIII. E-MRS 2011 Fall Meeting (Warsaw, Poland, September, 2012).

75. R.I. Eglitis, Ab initio calculations of the ABO_3 perovskite (001), (011) and (111) surfaces including bulk and surface F centers and Nb impurity segregation towards the $SrTiO_3$ surface. – Abstract: C-VI-2.

76. D. Fuks, E.A. Kotomin, A. Weizman, Yu.A. Mastrikov, M.M. Kuklja, and J. Maier, Ab initio thermodynamic study of phase competition in ABO_3-type multicomponent solid solutions. – Abstract: C-XI-2.

77. E.A. Kotomin, R. Merkle, Yu.A. Mastrikov, M.M. Kuklja, D. Fuks, and J. Maier, First principles calculations of defects in ABO_3 perovskites: applications for oxygen permeation membranes and SOFC cathodes. – Abstract: C-XI-3.

78. A.I. Popov, V. Pankratov, E. Klotins, L. Shirmane, V. Dimza, M. Antonova, M. Livinsh, and A. Kotlov, VUV synchrotron radiation spectroscopy of PLZT ceramics. – Abstract: C-31.

79. A.I. Popov, V. Pankratov, V. Bratus, and A. Kotlov, Electronic excitation and luminescence of pure and neutron-irradiated 3C-SiC. – Abstract: E-23.

80. R.I. Eglitis, Towards a practical rechargeable 5 V Li ion battery. – Abstract: F-XII-5.

81. A.I. Popov, V. Savchyn, V. Pankratov, V.T. Adamiv, Ya.V. Burak, and I.M. Teslyuk, VUV synchrotron radiation spectroscopy of $Li_2B_4O_7$ glass ceramics. – Abstract: F-32.

82. Yu.F. Zhukovskii, J. Kazerovskis, S. Piskunov, and S. Bellucci, Ni filament encapsulated inside single-walled carbon nanotubes: Predictions from first principles. – Abstract: G-3.

83. E. Blokhin, E.A. Kotomin, D. Gryaznov, R.A. Evarestov, and J. Maier, Confinement effects for point defects in perovskite ultrathin films. – Abstract: I-I-5.

84. R.I. Eglitis, H. Shi, R. Jia, L. Yue, and X. He, Ab initio calculations for the H centers in SrF_2 as well as surface H centers and F centers aggregation in BaF_2 and CaF_2. – Abstract: I-IX-3.

85. Yu.F. Zhukovskii, S. Piskunov, O. Lisovski, J. Kazerovskis, and J. Begens, Ab initio calculations of point defects in inorganic nanotubes. – Abstract: L-VII-1.

86. M.M. Kuklja, D. Fuks, O. Sharia, Yu.A. Mastrikov, and E.A. Kotomin, Vacancy-stabilized complex perovskites for SOFC applications. – Abstract: L-VII-2.

87. R.I. Eglitis, H. Shi, L. Chang, R. Jia, and Y. Wang, Ab initio calculations of hydroxyl impurities in CaF_2 and BaF_2. – Abstract: L-VII-3.

88. E. Klotins and G. Zvejnieks, Quantum chemical study of electron-phonon interactions in crystals. – Abstract: L-15.

XIX. 8th International Conference on Luminescent Detectors and Transformers of Ionizing Radiation (Halle, Germany, September, 2012).

89. V. Pankratov, A.I. Popov, L. Shirmane, A. Kotlov, G.A. Bizarri, A. Burger, P. Bhattacharya, E. Tupitsyn, E. Rowe, V.M. Buliga, and R.T. Williams, Luminescence of pure and europium doped SrI_2 and BaI_2, under VUV and x-ray excitation. - Abstracts: p. O-Mon-08.

90. I.M. Bolesta, I. Karbovnyk, S. Velgosh, I. Rovetsky, V. Pankratov, and A.I. Popov, Optical and AFM Characterization of Bismuth Nano-clusters embedded in CdI_2 Crystals. - Abstracts: p. P-Tue-54.

91. L. Shirmane, A.I. Popov, V. Pankratov, A. Lushchik, V.E. Serga, L.D. Kulikova, and A. Kotlov, Comparative Study of the Luminescence Properties of Macro Nanocrystalline MgO Using Synchrotron Radiation. - Abstracts: p. P-Tue-60.

92. A.I. Popov, J. Zimmermann, V. Pankratov, G.J. McIntyre, and H. von Seggern, Evaluation of Luminescent Properties of Neutron Image Plates. - Abstracts: p. P-Thu-61.

XX. 14th International IUPAC Conference on High Temperature Materials Chemistry, HTMC-14 (Beijing, China, September, 2012).

93. A. Weizman, D. Fuks, D. Gryaznov, E.A. Kotomin, Ab initio study of phase transformations in $(La_x,Sr_{1-x})CoO_3$: Beyond regular solid solutions.

XXI. 15th International Conference of Radiation Physics and Chemistry of Condensed Matter (Tomsk, Russia, September, 2012).

94. F.U. Abuova, A.B. Useinov, A.T. Akilbekov, E.A. Kotomin, S.Piskunov, First-principles calculations of radiation defects in magnesium fluorite, Abstracts, p.8-9.

XXII. The XVIIIth International Seminar on Physics and Chemistry of Solids (Lviv, Ukraine, September, 2012).

95. O.I. Aksimentyeva, V.P. Savchyn, P.Yu. Demchenko, I.Ye. Opaynych, Yu.Yu. Horbenko, P.V. Savchyn, and A.I. Popov, Luminescent properties and stucture of the hybrid composits based on BaZro3 nanocrystals in the polymer matrix.

XXIII. XIII Ukrainian-Polish symposium Theoretical and Experimental Studies of Interfacial Phenomena and their Technological Applications (Kyiv, Ukraine, September, 2012).

96. O.I. Aksimentyeva, V.P. Savchyn, V.P. Dyakonov, S. Piechota, I.Ye. Opaynych, Yu.Yu. Horbenko, and A.I. Popov, Hybrid polymer-magnetic nanocomposites with conductive and luminescent functions.

XXIV. International Workshop on Nanoscience and Nanotechnology, n&n-2012 (Frascati, Italy, October, 2012).

97. S. Piskunov, Yu.F. Zhukovskii, J. Kazerovskis, and S. Bellucci, First principles calculations of Ni filament encapsulated inside single-walled carbon nanotube. - Abstracts: p. 37-38.

98. Yu.N. Shunin, Yu.F. Zhukovskii, V.I. Gopeyenko, N. Burlutskaya, T. Lobanova-Shunina, and S. Bellucci, Nanocarbon electromagnetics for nanosensor applications. - Abstracts: p. 63-66.

99. S. Piskunov, Yu.F. Zhukovskii, O. Lisovski, J. Begens, and S. Bellucci, Ab Initio calculations of C-, N-, S-, and Fe-doped TiO_2 and SrTiO3 nanotubes for photocatalytical water-splitting application. - Abstracts: p. 117-118.

100. S. Piskunov, Yu.F. Zhukovskii, J. Kazerovskis, P.N. Dyachkov, and S. Bellucci, Electronic structure of BN nanotubes containing point defects: Predictions from first principles. - Abstracts: p. 119-120.

XXV. First Baltic School on Application of Neutron and Synchrotron Radiation in Solid State Physics and Material Science, BSANS-2012 (Riga, Latvia, October, 2012).

101. Yu.F. Zhukovskii and S. Piskunov, Ab initio simulations on perefect and defective inorganic nanotuves and nanowires. - Abstracts: p. 18

102. C. Balasubramanian, S. Bellucci, M. Cestelli Guidi, A. Ivanov, A.I. Popov, H. Schober, V. Savchyn, and Yu.F. Zhukovskii, A comprehensive study and analysis of aluminium nitride

nanostrucures by inelastic neutron scattering and xanes, ftir and luminescence spectroscopies. - Abstracts: p.28

103. A. Gopejenko, Yu.F. Zhukovskii, P. Vladimirov, E.A. Kotomin, Yu. Mastrikov, and A. Möslang, Ab initio modelling of th yttrium and oxigen nanoparticle formation inside FCC iron latice for ods steels development. - Abstracts: p. 30.

104. A. Jersova, A.I. Popov, V. Pankratov, L. Shirmane, K.A. Gross, and A. Viksna, Synchrotron radiation luminescence spectroscopy of strontium substituted hydroxyapatites. - Abstracts: p. 32.

105. I. Karbovnyk, P. Savchyn, A. Voloshinovskii, M. Cestelli Guidi, C. Mirri, and A.I. Popov, $LaPO_4$ IR spectra: nanoparticles vs. bulk. - Abstracts: p. 35.

106. I. Karbovnyk, P. Savchyn, A. Huczko, M. Cestelli Guidi, C. Mirri, and A.I. Popov, FTIR studies of silicon carbide nanostructures. - Abstracts: p. 36.

107. I. Karbovnyk, I. Bolesta, V. Savchyn, M. Cestelli Guidi, and A.I. Popov, Infrared characterization of pure and doped cadium iodide crystals. - Abstracts: p. 37.

108. E. Klotins and G. Zvejnieks, Radiation field-electron-phonon interaction in the Hartree-Fock model. - Abstracts: p. 38.

109. A. Kuzmin, V. Pankratov, A. Kalinko, A. Kotlov, L. Shirmane, and A.I. Popov, UV-VUV synchrotron radiation spectroscopy of $NiWO_4$. - Abstracts: p. 42.

110. P. Merzlyakov, G. Zvejnieks, V.N. Kuzovkov, E.A. Kotomin, K.D. Li, T.H. Ding, and L.M. Wang, Quantitaative analysis of void lattice formation in CaF_2. - Abstracs: p. 43.

111. P. Merzlyakov, G. Zvejnieks, V.N. Kuzovkov, and E.A. Kotomin, Modelling of void lattice self-organization in CaF_2. - Abstracts: p. 44.

112. V. Pankratov, L. Shirmane, A. Kotlov, and A.I. Popov, Synchrotron based VUV spectroscopy of YA nano- and single crystals. - Abstracts: p. 46.

113. A.I. Popov, V. Pankratov, S. Piskunov, L. Shirmane, E.A. Kotomin, and A. Kotlov, Luminiscence of Fe and Nb doped $SrtiO_3$ monocrystals under VUV synchrotron radiation. - Abstracs: p. 47.

114. A.I. Popov, V. Pankratov, V. Bratus, G. Chikvaidze, A.Moskina, and A. Kotlov, Electronic excitation and luminescence of pure and nuetron-irradiated 3C-SiC. - Abstracts: p. 48.

115. A.I. Popov, J. Zimmermann, V. Pankratov, G.J. McIntyre, and H. von Seggern, Luminescent properties of neutron image plates. - Abstracts: p. 49.

116. A.I. Popov, V. Pankratov, E. Klotins, L. Shirmane, V. Dimza, M. Antonova, M. Livinsh, and A.Kotlov, VUV synchrotron radiation spectroscopy of PLTZ ceramics. - Abstracts: p. 50.

117. V. Savchyn, A. I Popov, O. Aksimentyeva, Y. Horbenko, P. Savchyn, and V. Pankratov, Cathodoluminescence characterization of polystyrene - $BaZrO_3$ hybrid composites. - Abstracts: p. 52.

118. L. Shirmane, V. Pankratov, A.I. Popov, A. Kotlov, and W. Strek, Luminescence of $MgAl_2O_4:Cr^{3+}$ nanocrystals under synchrotron radiation. - Abstracts: p. 53.

119. L. Shirmane, A.I. Popov, V. Pankratov, A. Lushchik, V.E. Serga, L.D. Kulikova, and A. Kotlov, Comparison of luminescence properies of macro and nanocrystalline MgO using synchrotron radiation. - Abstracts: p. 54.

120. L. Shirmane, A. Kuzmin, A.I. Popov, and V. Pankratov, Raman scattering of nano and macrosized europium doped YVO_4. - Abstracts: p . 55.

121. P. Zhgun, D. Bocharov, S. Piskunov, A. Kuzmin, and J. Purans, Electronic structure and lattice dynamics of ScF_3 from firts-princiles LCAO calculations. - Abstracts: p. 58.

***XXV. International Workshop „Hydrogen and Fuel Cells in Research and Applications: facing to Latvia" (Riga, Latvia, October 2012)**.*

122. Yu.F. Zhukovskii and S. Piskunov, "Catalysts on the surface of the oxide nanotubes - calculations from the first principles".

XXVI. Fall MRS Meeting (Boston, USA, November, 2012)

123. R. Merkle, L. Wang, A. Wedig, Yu.A. Mastrikov, E.A. Kotomin, and J. Maier, "Oxygen exchange kinetics on solid oxide fuel cell cathode materials - mechanistic interpretation and the importance of defects". Abstracts: I1.05

124. M. Kuklja, E.A. Kotomin, R. Merkle, Yu.A. Mastrikov, and J. Maier, "Comparative analysis of oxygen vacancy diffusion in LSCF and BSCF perovskite solid solutions: Ab initio modeling". Abstracts: I9.17.

125. M. Kuklja, D. Fuks, O. Sharia, Yu.A. Mastrikov, and E.A. Kotomin, "Degradation and stability of complex perovskites for energy applications". Abstracts: I2.02.